

Abstracts for the 2023 CBTH Annual Sponsor Meeting

Principal Investigator:

Paul Mann, University of Houston (UH)

With abstracts from:

Mohamed Abdelfatah, UH

Jumoke Akinpelu, UH

Ruth Beltran, UH

David Castro, Universidade Federal do Rio Grande do Norte

Sharon Cornelius, UH

Tarek Galhom, UH (now at University of Bergen)

José Miguel Gorosabel Araus, UH

Jose-Luis Granja-Bruña, Complutense University of Madrid

Md Nahidul Hasan, UH (now at BP)

Mei Liu, UH (now at TGS)

Paul Mann, UH

Daniel Maya, UH

Alanny Melo, Universidade Federal do Rio Grande do Norte

Diógenes C. Oliveira, Universidade Federal do Rio Grande do Norte

Chesney Petkovsek, UH

Juan Pablo Ramos Vargas, UH

Md Upal Shahriar, UH

Kenneth Shipper, UH

Jeff Storms, UH



September 1, 2022 – August 31, 2023

Contents

Contents.....	ii
Introduction and database.....	4
1. Introduction to the volume by Paul Mann.....	5
2. Overview of the CBTH GIS database for sponsors by José Miguel Gorosabel Araus and Jeff Storms	7
3. CBTH website, integration with Geopost, and deliverables to sponsors by Jeff Storms	9
Gulf of Mexico, Permian Basin, and the Caribbean.....	11
4. CBTH advances in understanding major hydrocarbon basins from West Texas to Guyana by Paul Mann	12
5. Integration of refined geothermal gradients of the Delaware basin, west Texas, with observations from gravity and 2D and 3D seismic reflection data by Chesney Petkovsek	18
6. Late Cretaceous-Recent tectonostratigraphic evolution of the Yucatan back-arc basin, northern Caribbean Sea by Juan Pablo Ramos Vargas	21
7. Crustal structure of the Bahamas platform and implications for basin modeling by Kenneth Shipper	24
8. Basin modeling of the Eocene to Present forearc San Pedro Basin (Dominican Republic offshore) by José Miguel Gorosabel Araus, Paul Mann, and Jose-Luis Granja-Bruña	26
South America.....	28
9. Crustal structure in the Colombian Basin and its control on the distribution of potential source rock and play fairways in deep and ultra-deep waters of the Caribbean by Juan Pablo Ramos Vargas	29
10. Control of crustal thickness, type, and burial history on heat flow and petroleum basin modeling of the Guyana-Suriname rifted-passive margin by Kenneth Shipper	32
11. The Barreirinhas Basin: An unexplored frontier with significant potential in the Brazilian equatorial margin by José Miguel Gorosabel Araus, Paul Mann, Alanny Melo, David Castro, and Diógenes C. Oliveira	34
12. Syn-rift and salt depositional thicknesses in the rift zones of the Santos-Campos-Espirito Santo salt basin, Brazil, resulting from the southwestward tilting of the basement by Sharon Cornelius	36
13. Exploring the external kitchen of the Campos basin, Offshore Brazil using cutting-edge 3D seismic data by Ruth Beltran	38
14. Transferring deepwater play concepts from hydrocarbon discoveries in Namibia to its conjugate margin in Argentina by Daniel Maya	41
West Africa.....	44
15. Tectonic controls on Mesozoic source rock thermal maturity of the 3500-km-long, rifted-passive Atlantic margin of Morocco by Paul Mann, Md Nahidul Hasan, and Tarek Galhom ..	45
16. Crustal structure and hydrocarbon potential of the non-volcanic and volcanic, rifted-passive margins of Mauritania by Md Upal Shahriar	51

17. Hydrocarbon prospectivity of deeply-buried Early Cretaceous rifts of the western deepwater area of the Niger delta, Nigeria by Jumoke Akinpelu	53
18. 3D and 2D mapping and basin modeling of the Rio Muni Basin, offshore Equatorial Guinea by José Miguel Gorosabel Araus.....	55
19. Relationships between Red Sea opening directions, crustal types and thicknesses, evaporite distribution, and hydrocarbon potential by Mohamed Abdelfatah	57
References.....	60

INTRODUCTION AND DATABASE

- Chapter 1 - Introduction to the volume by Paul Mann
- Chapter 2 - Overview of the CBTH GIS database for sponsors by José Miguel Gorosabel Araus and Jeff Storms
- Chapter 3 - CBTH website, integration with Geopost, and deliverables to sponsors by Jeff Storms

1. Introduction to the volume

Paul Mann, CBTH Project Principal Investigator, Professor of Geology, University of Houston

The goal of the three-year Conjugate Basins, Tectonics, and Hydrocarbons (CBTH) Project Phase VI (September 2020 – August 2023) was to continue and expand upon the research activities and focus of Phases I through V (September 2005 – August 2020). The main goal of CBTH Phase VI will be to continue to provide our industry sponsors with a fully integrated, web-based, digital surface and subsurface synthesis of a hydrocarbon-rich study area that includes on- and offshore areas of the Gulf of Mexico, the Caribbean, northern South America, Africa, and Atlantic conjugate margins.

A main focus of Phase VI was to expand our GIS and reference compilations for all these areas, seek opportunities to access subsurface data from key areas, and build regional maps of key tectonosequences that establish the regional basinal and stratigraphic framework that was then used to create quantitative basin models predicting source rock maturity and hydrocarbon distribution. A major theme of Phases V through VI is the study of now widely separated conjugate Gulf of Mexico and circum-Atlantic margins in the context of their original and shared, pre-rift ancestry. We have found that these data-driven types of activities are of great benefit to our sponsors and can be done at relatively modest costs given that our compilation effort is carried out by undergraduate and graduate students at the University of Houston.

Since the start of the CBTH Project in 2005, our project has received financial support from a total of 31 oil and gas exploration companies that include are four current sponsors for Phase VI, Year 3, Phase VI from September 1, 2022 to August 31, 2023: Petrobras, Woodside (formerly BHP Billiton), TotalEnergies, and Hess. We thank all past and present sponsors for their support and in many cases hiring the students for summer internships and full-time jobs. We thank our current data providers TGS and Geox-MCG for their long-term support of CBTH along with all previous data providers dating back to 2005. We also thank the many software companies that provide our essential software at either at no cost or a reduced academic rate.

As university researchers, publications and presentations at industry and academic conferences remain a top priority of the CBTH Project. A complete list of CBTH theses, presentations, and publications dating back to the start of the project in 2005 can be found on our website at <http://cbth.uh.edu/contributions.php>

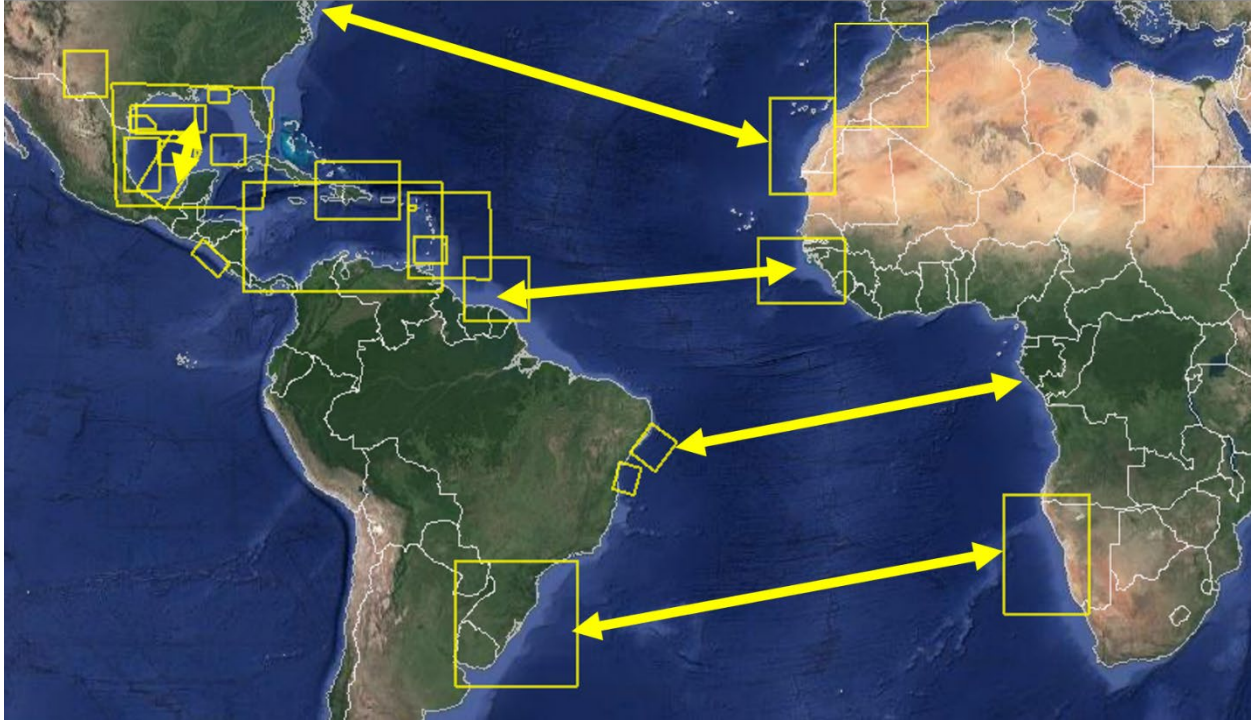


Figure 1. Key CBTH study areas along the conjugate margins of South America, Central America, North America, and Africa.

2. Overview of the CBTH GIS database for sponsors

José Miguel Gorosabel Araus, Research Associate 1, University of Houston
Jeff Storms, Project Consultant, University of Houston

The CBTH database is an extensive compilation of data that focus on hydrocarbon related information that are assembled by researchers with the CBTH Project. The database began at UT Austin in 2005 with the support of a consortium of companies. The CBTH database aims to: 1) provide the latest information and data to CBTH sponsors to aid them in their exploration efforts in the CBTH study area; 2) collect multiple datasets to build regional GIS syntheses and maps for the CBTH study area within which a critical source of new maps and information are the various student projects at UH and UiS; and 3) generating regional tectonic models that can be validated from data in the CBTH database.

CBTH partnered with Geopost (now part of Katalyst Data Management) for archiving CBTH database and online access to the sponsors. The database consists of CBTH research projects, public data, and database compilations from literature including journal articles, conference proceedings and presentations, and theses. The web-based data portal is an application custom-built on the ArcGIS Online platform that enables the sponsors to visualize the data without the having to load the data, thus provide easy data access to sponsors anywhere with internet connection. The interface is user-friendly and all the layers can be toggled on and off for viewing.

The following list summarizes data being delivered to sponsors through the web-based Geopost portal/FTP:

- GIS vector data: We maintain a GIS database of useful information compiled from various resources including CBTH research projects, public data sources, and scientific publications. The database include GIS vector features such as wells, cores, outcrops, stratigraphic columns, detrital zircon data, radiometric ages, thermochronology ages, oil and gas seeps, faults, seismic lines, and cross sections. Detrital zircon data has been one of the popular products that help to reconstruct ancient sedimentary pathways, evaluate sediment source areas, and reconnect long-severed tectonic relationships. Among all modes of clastic transport, fluvial transport is most often called upon to move large populations of detrital zircons great distances. Our compilation contains more than 55,000 records of detrital zircon data.
- GIS raster data: We compile public maps and generate new maps in our CBTH research projects. These include the topography and bathymetry, satellite free air gravity anomalies, magnetic anomalies, stratigraphic and lithospheric surfaces that we mapped from seismic data grids and public data sources, sediment thicknesses, processed potential fields anomalies, crustal thicknesses, and gravity inversion studies. All the CBTH mapped digital grids have been loaded onto the Geopost web portal with over 14,000,000 km² total areal coverage, these data can be downloaded from <https://uh.geopostenergy.com/FileManager/>

GIS vector data compilations

- Wells
- Cores
- Outcrops
- Stratigraphic columns
- Detrital zircons
- Radiometric ages
- Thermochronology
- Seeps
- Faults
- Seismic lines
- Cross sections

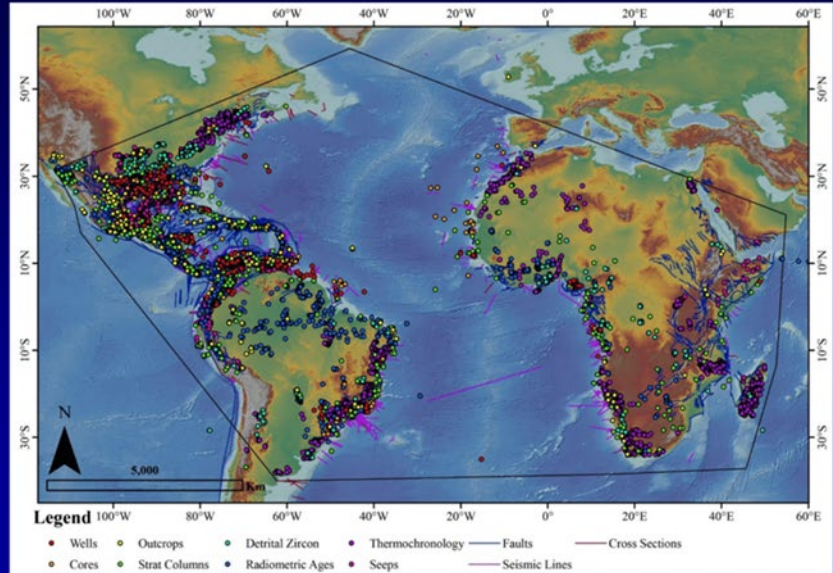


Figure 1. Snapshot of CBTH vector data compilations.

GIS raster data compilations

- Topography
- Bathymetry
- Satellite free air gravity anomalies
- Magnetic anomalies
- Stratigraphic surfaces
- Basement surfaces
- Moho surfaces
- Crustal thickness

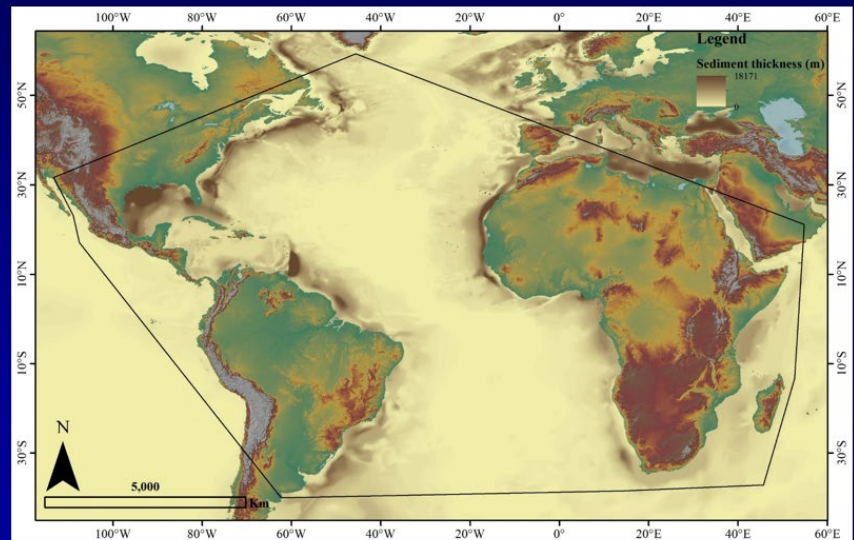


Figure 2. Snapshot of CBTH raster data compilations. Map shows sediment thickness in the CBTH study area.

3. CBTH website, integration with Geopost, and deliverables to sponsors

Jeff Storms, Project Consultant, University of Houston

Sponsors of the Conjugate Basins, Tectonics, and Hydrocarbons (CBTH) Project receive access to the CBTH website (<http://cbth.uh.edu>). The site is composed of two key directories:

- Publicly accessible directory contains project researcher bios, proposals, recent news, selected publications, lists of upcoming meetings, the full CBTH contributions list, and awards.
- Sponsors Only directory contains links to download all CBTH data releases, theses, presentations, and publications. This password-protected directory is exclusively available to active project sponsors and is updated regularly to reflect new materials. This section also contains a link to Geopost, our online data visualization tool which allows sponsors to view and map all current and previous CBTH data.

In addition to GIS database updates, key content additions to the CBTH database and website this year include recently completed theses, selected posters and presentations, and recent and in-progress publications by CBTH students and personnel. These materials will also be included in the “CBTH-2023” FTP data release.

Sponsors will receive this year’s project deliverables via FTP, or via a hard disk upon request. These deliverables are also available through the Geopost data portal, which is a browser-based mapping and visualization application. For this year’s end-of-phase atlas (available in Spring 2024), we will provide a large-scale, map-based atlas covering all CBTH research in Phase VI.

As of September 2023, students and researchers for the CBTH Project have contributed to 75 PhD, MSc, and BSc theses, 743 presentations, and 144 completed publications during the course of Phases I-VI (Figure 1).

Since 2018, CBTH personnel have been working with Geopost to populate the data portal with all CBTH deliverables going back to Phase I in 2005. During this process, we have worked to ensure that all relevant materials are posted in the highest quality possible. We have also worked to eliminate redundancy by consolidating outdated materials, merging datasets, and comparing materials to our ongoing Contributions List.

On social media, the CBTH Project is active on LinkedIn, which we use to connect with sponsor representatives, colleagues, and current, former, and prospective students. Using LinkedIn, interested parties can contact CBTH students and researchers regarding project information, consulting services, job opportunities, and more.

All sponsors who have made this year's payment on-time will their new CBTH website passwords, Geopost login credentials, and FTP credentials following the CBTH year-end meeting. This grants access to all CBTH materials from Phases I-VI through the website, our secure FTP, and access to the Geopost data portal. These passwords are confidential and will only be submitted to the designated company representatives. Sponsor representatives may share these credentials with their co-workers, but we ask that representatives respect the security of his or her company's login information.

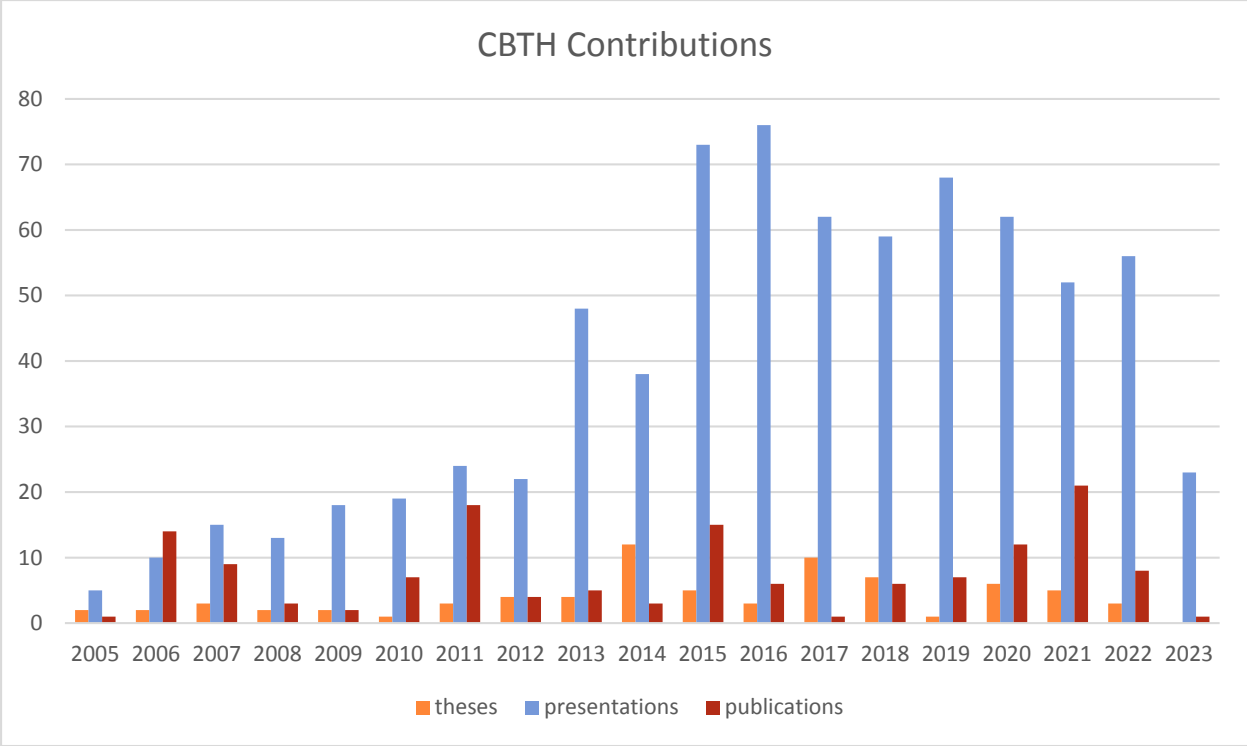


Figure 1. Histogram of all CBTH-affiliated theses, presentations, and publications since the beginning of the project in 2005 through September 2023.

GULF OF MEXICO, PERMIAN BASIN, AND THE CARIBBEAN

- Chapter 4 – CBTH advances in understanding major hydrocarbon basins from West Texas to Guyana by Paul Mann
- Chapter 5 – Integration of refined geothermal gradients of the Delaware basin, west Texas, with observations from gravity and 2D and 3D seismic reflection data by Chesney Petkovsek
- Chapter 6 – Late Cretaceous-Recent tectonostratigraphic evolution of the Yucatan back-Arc basin, northern Caribbean Sea by Juan Pablo Ramos Vargas
- Chapter 7 - Crustal structure of the Bahamas platform and implications for basin modeling by Kenneth Shipper
- Chapter 8 - Basin modeling of the Eocene to Present forearc San Pedro Basin (Dominican Republic offshore) by José Miguel Gorosabel Araus, Paul Mann, and Jose-Luis Granja-Bruña

4. CBTH advances in understanding major hydrocarbon basins from West Texas to Guyana

Paul Mann, CBTH Project Principal Investigator, Professor of Geology, University of Houston

In this overview talk, I review the progress of major hydrocarbon basins across the CBTH study area, including the Permian basin of West Texas and New Mexico, the Gulf of Mexico basin with a focus on the Campeche basin of southern Mexico, the Colombian-Venezuelan basin of the Caribbean Sea, and the Guyana-Suriname area of northeastern South America. Except for Brazil, these four regions are currently the most productive hydrocarbon basins of the Western Hemisphere (Figure 1.).

The Permian basin records a major, northward and northwestward-verging collision between the northern margin of South America (the Yucatan block) during the Pennsylvanian and Permian (Figure 2). This continent-continent collisional event terminated sedimentation along the former Paleozoic passive margin almost synchronously in a zone of thrust deformation extending from the Arkoma basin in the east to the Orogrande basin to the west. Comparison of the start and end times for the most rapid subsidence rates marking the period of orogenic activity revealed only a very slight east to west younging which indicates that collision of the South American plate occurred almost synchronously across a broad zone that transitioned to the “Ancestral Rockies” in the continental interior to the north. The Delaware basin exhibits the highest total subsidence of 8 km of the entire orogenic belt, likely due to its position adjacent to the orogenic belt and downdip of eroding areas from the orogenic belt to the south. Our work in the Permian basin is to use gravity and magnetic data to constrain its underlying crustal types and properties better, to define the syn-tectonic Wolfcamp Formation in three dimensions using 2D and 3D seismic reflection data sets, and to refine the basin model by improving the regional control on heat flow.

In the Gulf of Mexico, we have inverted regional gravity data sets to map variations in crustal thickness related to the two-phase opening of the Gulf of Mexico during an early continental rifting phase from the Late Triassic to Early Jurassic and a Late Jurassic rifting and oceanic spreading event that produced a large area of oceanic crust (Figure 3). Our work has focused on using gravity and magnetic data integrated with 2D seismic reflection and refraction lines to define the continent-ocean boundaries and to map the semi-continuous marginal rift system that borders the area of the oceanic crust (Figure 4). For the Campeche area, we have carried out basin modeling of the Jurassic sedimentary rocks within the rift to show that the source rocks are mature and expelling oil and gas (Figure 4). Our maturity prediction is consistent with the presence of oil and gas seeps in this area.

In the Venezuelan and Colombian basin of the Caribbean Sea, we have used basin modeling based on analyzed late Cretaceous samples from DSDP wells to show that mature Cretaceous source rocks exist in an elongated area to the active subduction zone between the Caribbean Sea and South America (Figure 5). Maturity is related to deep burial beneath the 8-km-thick overburden of the Magdalena deepsea fan. We predict updip migration of these hydrocarbons into large stratigraphic traps.

In Guyana, we analyzed vintage 2D seismic and reflection data from 2009-2011 to identify the Berbice submarine fan and then carried out 2D modeling of vintage wells to show maturity of presumed Cenomanian-Turonian source rocks similar to those of Venezuela and Trinidad. We

compare our early results based on sparse vintage data with the results from more recent work based on deeper wells and 3D seismic reflection data (Figure 6).

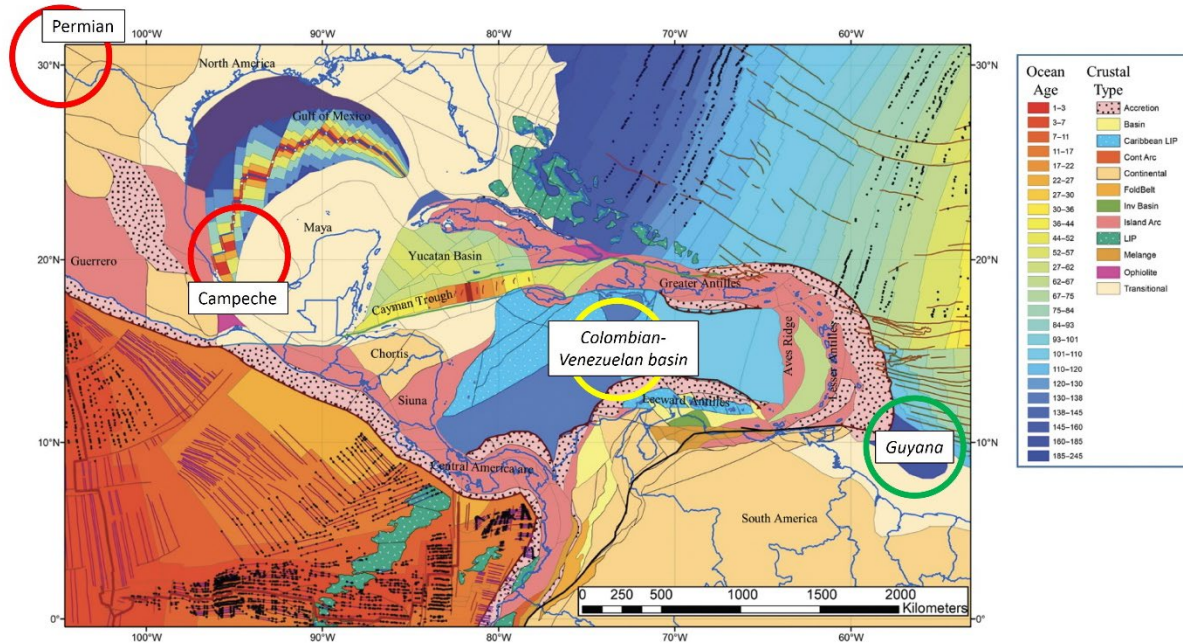


Figure 1. Plate tectonic model from Escalona et al. (2021) at present-day showing the different rigid blocks classified into various geological groups depending on their crustal type and origin. Circles indicate the known or proposed hydrocarbon basins reviewed in this talk: 1) Permian basin of west Texas; 2) Campeche Basin of southwestern Gulf of Mexico; 3) Colombia-Venezuela Basin of the Caribbean Sea; and 4) Guyana Basin of northeastern South America.

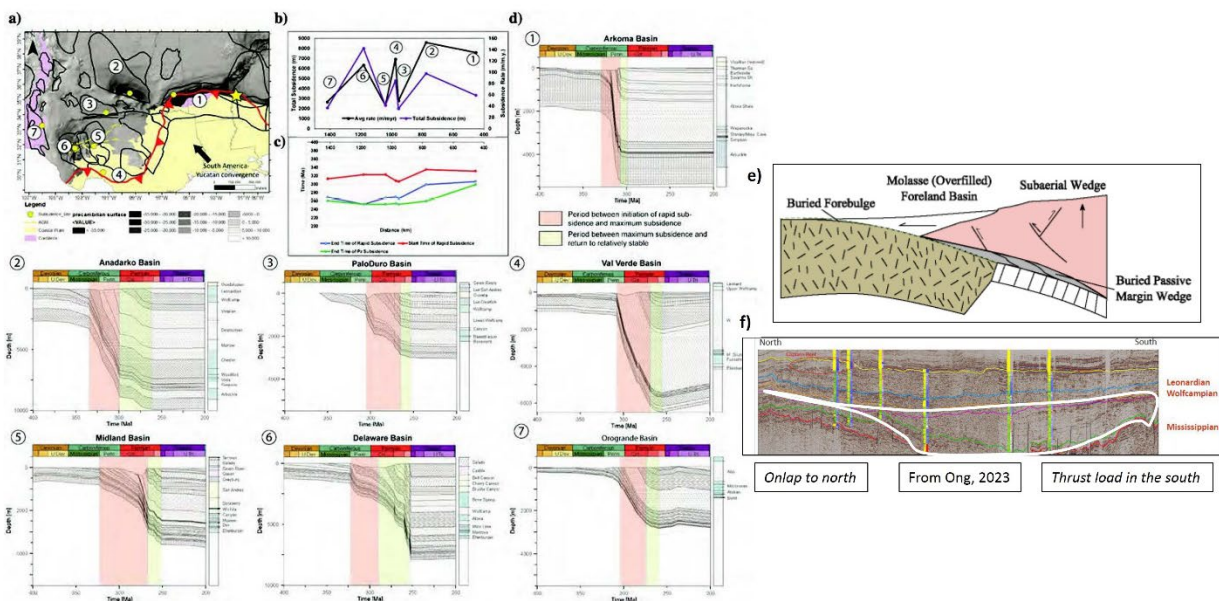


Figure 2. A) Location of the representative wells of seven sedimentary basins along the Marathon-Ouachita orogenic belt and part of the Ancestral Rocky Mountains system, including the (1) Arkoma Basin, (2) Anadarko Basin, (3) Palo Duro Basin, (4) Valverde Basin, (5) MB, (6) DB, and (7) Orogrande Basin from Zhang et al. (2021). B) Plot showing the maximum subsidence rate for the seven basins compared to their estimated distance from the easternmost location where continental collision is thought to have initiated. C) Plot showing the time of the most rapid subsidence initiation and the maximum subsidence rate for the seven basins versus the estimated distance from where continental collision began (labeled as a star in A). D) Subsidence analysis for the seven basins showing the period from the initiation of rapid subsidence and reaching their maximum subsidence rate followed by the end of rapid subsidence and with an eventual return to post-orogenic, basin stability. E) Generalized model for a foreland basin showing the orogenic load to the right and the flexural response of the continental crust with the formation of a foreland basin to the left. F) North-south regional seismic line through the Delaware basin from Ong (2023) showing the syn-orogenic, organic-rich, Wolfcamp marine shale filling the depression produced by overthrusting and plate flexure.

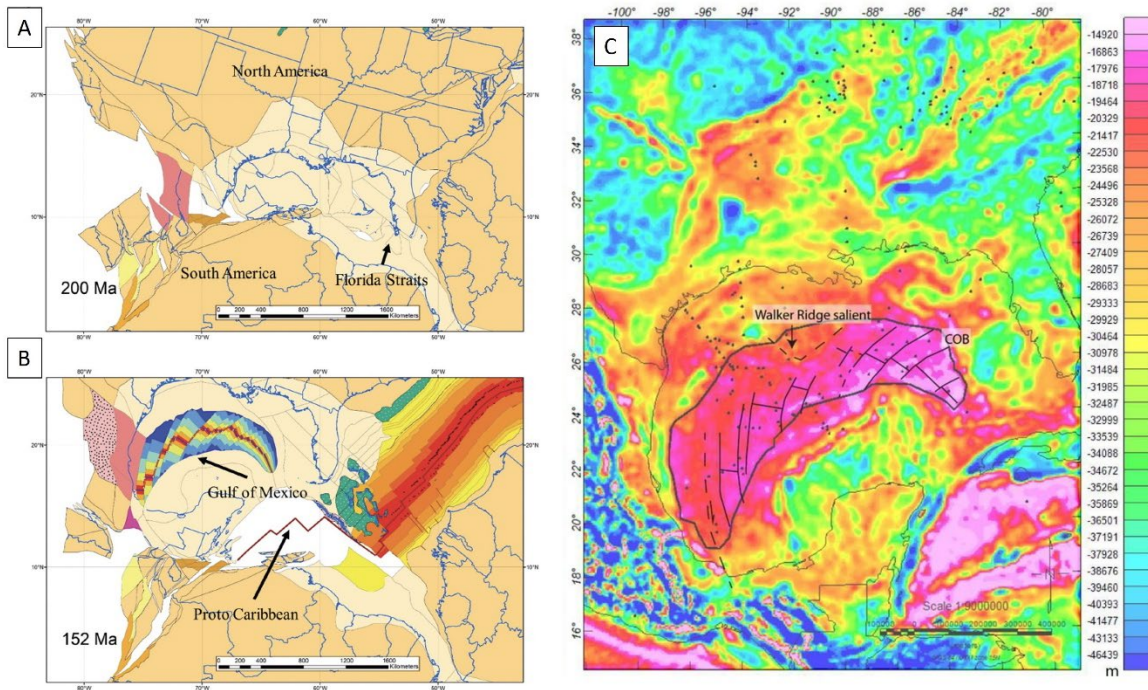


Figure 3. Jurassic development of the Gulf of Mexico at 200 Ma (A) and 152 Ma (B) from Escalona et al. (2021). The counterclockwise rotation of the Yucatan block resulted in the formation of the oceanic crust underlying the deep Gulf of Mexico. C) Moho surface derived from constrained 3-D gravity structural inversion by Liu (2021). The black dots are refraction stations from compiled literature that were used for Moho corrections. The COB is defined by the crustal thickness less than 10 km except in the NW GOM where the COB is adjacent to a northeast-trending deeper Moho expression. The extinct spreading center and fracture zones are compiled from Lin et al. (2019).

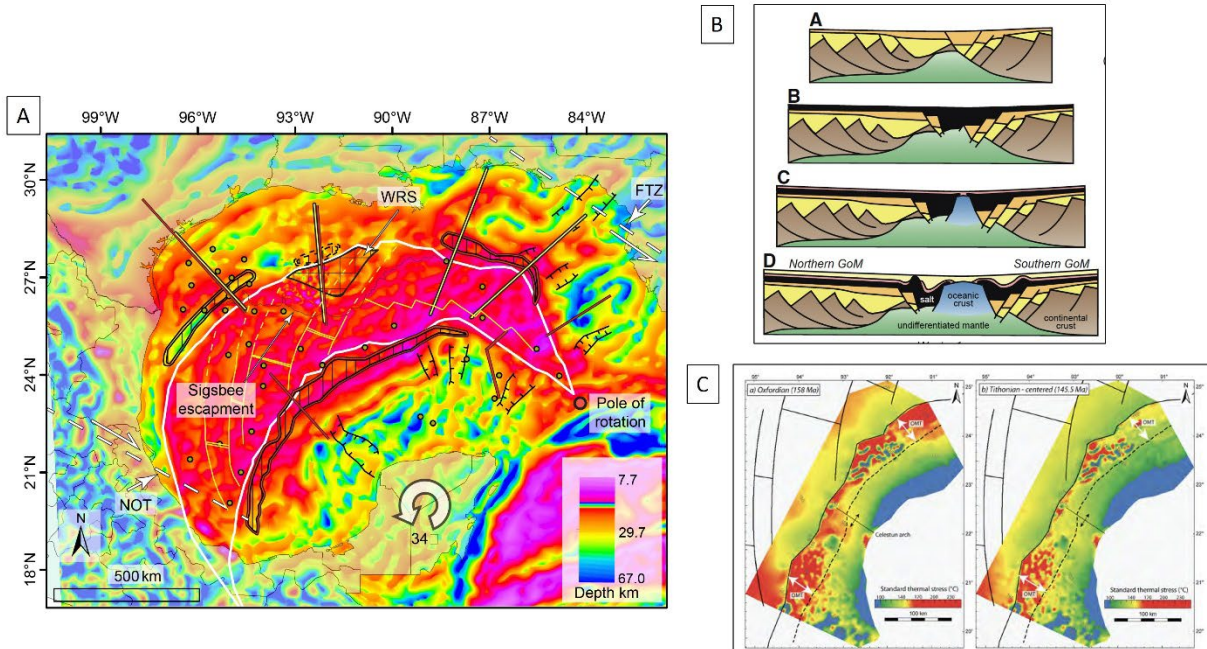


Figure 4. A) Summary of the constraints used by Bugti (2022) for locating the continent-ocean boundary in the Gulf of Mexico shown by the white line. The base map is the crustal thickness map based on 3D gravity inversion by Liu (2021). Marginal rifts are shown in double black polygons filled with vertical lines and were compiled from Liu (2021). Seismic lines crossing the proposed COB were compiled from various sources. The outline of the Walker Ridge Salient (WRS) now known to an elevation related to mobile salt. B) Schematic evolutionary cartoons from Rowan (2022) of the along-strike variation in the relative timing of late-stage rifting, early spreading, and salt deposition based on his interpretations of the continent-to-ocean transition in the western GOM with the latter assumed to be simultaneous (time stage 2) across the basin. The splitting of the central, salt-filled rift results in the marginal rifts observed adjacent to the oceanic crust in most areas of the GOM (cf. map in Figure 4). C) Standard thermal stress (STS) maps of the Campeche area of the southwestern GOM based on constant radiogenic heat production (RHP) per unit thickness of continental crust. RHP from the oceanic crust is assumed to be zero. (left) STS map for the Oxfordian source interval. (right) STS map for the Tithonian-centered source interval. Source intervals are mature within the more deeply buried marginal rift formed on rifted, continental crust with higher heat flow.

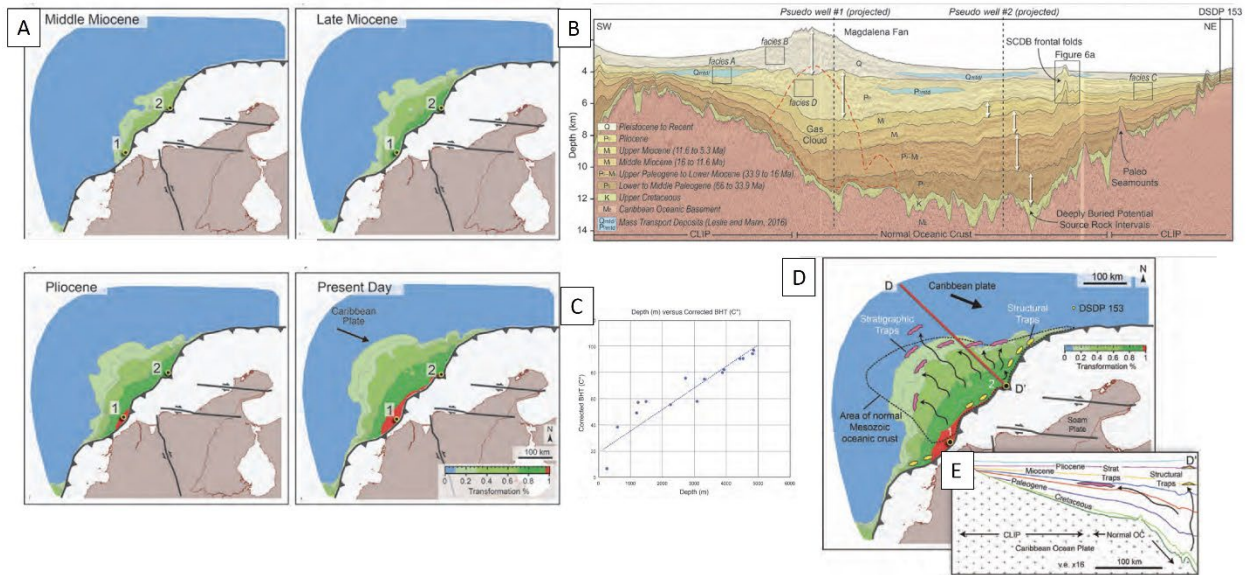


Figure 5. A) Depth to the top of the Caribbean oceanic crust (meters below sea level) from Leslie and Mann (2020). Seismic lines that map this horizon are shown as blue dashed lines. Pseudowell locations for basin modeling are positioned in the deepest part of the basin (numbered 1 and 2). Total sediment thickness shown in meters. B) Approximately 800 km long composite strike line A-A' along the southern boundary of the Colombian Basin parallel to the axis of the SCDB, comprising various vintages of depth-converted 2D seismic data. Stratigraphic and structural interpretation of the strike line. Stratigraphic ages from Upper Cretaceous denoted by color. Note the large depocenter associated with the Magdalena fan and the apparent southwestward stepping of the thickest portion of each unit from older to younger (the white arrows), due to the east-southeast movement of the Caribbean Plate relative to the mouth of the paleo-Magdalena River system. An area of poor imaging below Magdalena fan interpreted as a gas cloud (the red arrow). The top of the Caribbean Plate basement is recognized as a rugose reflection event, punctuated by high-relief (1–2 km) features interpreted as seamounts. The Caribbean Plate basement in the center of the figure is interpreted as a typical-thickness Mesozoic oceanic crust, bounded by thicker CLIP basement to the southwest and northeast. C) Corrected bottom-hole-temperature-versus depth relationship derived from three closely spaced wells proximal to the mouth of the Magdalena fan in Colombia. D) Summary of potential play types and migration pathways in the Colombian Basin. Map showing the present-day thermal maturity, migration pathways (curved arrows), and potential and inferred hydrocarbon traps. Stratigraphic traps are represented by the pink polygons and structural traps by the yellow ovals. E) Cross section through the “early kitchen” area showing potential migration pathways (the arrows) and possible hydrocarbon traps (the pink and yellow polygons).

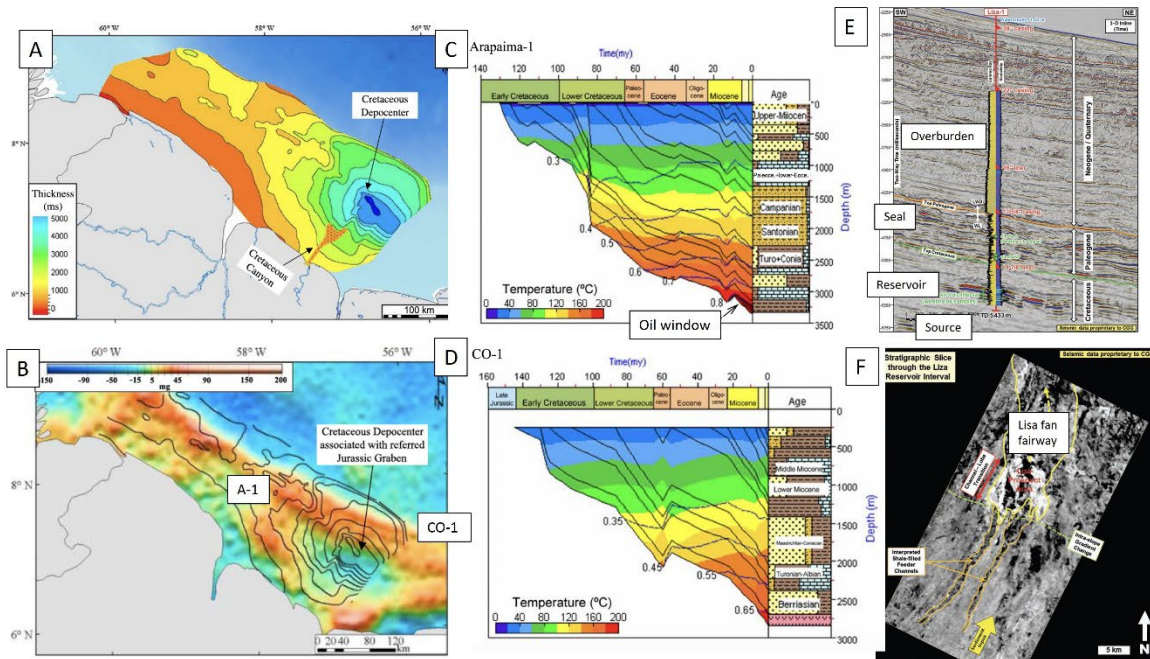


Figure 6. A) Regional isochron map of sequence 1 (Cretaceous). The map shows that the main depocenter developed in the southeastern Guyana Basin. The large Berbice canyon connects this depocenter with onland paleo drainage systems. B) Interpreted Cretaceous depocenter on the top of the free-air gravity, suggesting that the Cretaceous depocenter developed above a Jurassic rift. C) Burial history analysis of shelfal well Arapaima-1. D) Burial history analysis of shelfal well CO-1. E) Liza-1 well logs superimposed on a 3-D seismic inline at the well location from Price et al. (2021). F) Stratigraphic slice through the Liza reservoir interval with interpreted feeder channels, channel-lobe transition, and Liza depositional fairway.

5. Integration of refined geothermal gradients of the Delaware basin, west Texas, with observations from gravity and 2D and 3D seismic reflection data

Chesney Petkovsek, PhD Candidate, University of Houston and Callon Petroleum

In the first part of the study, I present a newly-calibrated and non-linear, temperature-depth function for the Delaware basin of west Texas that results in higher geothermal gradients than the previous estimates based on linear models (Figure 1). The resulting non-linear depth function is validated within a 4.2% error with measured bottom hole temperatures for the Wolfcamp source rock interval. The War-Wink Correction Method used in this study is calibrated to a high-quality temperature dataset from the eastern Delaware Basin that has been integrated into the regional dataset of 453 unique temperature measurements from 1,024 log headers within 140 wells penetrating Precambrian-to-Pennsylvanian age strata. BHT corrections are grouped into four thermal packages based on a regional 3D stratigraphic model that are then used to constrain four, interval-specific geothermal gradient maps for the entire Delaware Basin (Figure 2). Using this model, the average corrected geothermal gradient for the base of Wolfcamp – Precambrian interval is 21.7 °C/Km, the base of Bone Spring- base of Wolfcamp is 20.3 °C/Km, the base of evaporites-base of Bone Spring interval is 21.8 °C/Km, and the interval from surface – base of evaporites is 37.4 °C/Km.

Using the interval specific and non-linear model shown in Figure 2, I can explain localized heatflow variations and their geologic controls: 1) Lower geothermal gradients (15.5-21 °C/Km) and gas-oil-ratio figure values (1,000-12,000 scf/Bbl) from the Wolfcamp- Precambrian units overlie mafic intrusions inferred from gravity and magnetic surveys and confirmed by core data; 2) Higher geothermal gradients (21-25.9 °C/Km) and gas-oil-ratio values (12,000-30,000+ scf/Bbl) within Wolfcamp-Precambrian units overlie granitic provinces; and 3) localized thermal anomalies of up to 9 °C/Km occur within faulted blocks which overlie deeply-rooted fault system like the Grisham fault zone and Mi Vida fault block, creating discrete thermal regimes (Figure 3). The higher geothermal gradients and their geologic mechanisms provide a fundamental constraint for modeling the thermal history and hydrocarbon expulsion from the Wolfcamp source rock interval.

In the second part of the study, I use regional gravity and 2D and 3D seismic reflection data to illustrate the 3D geometry of the Delaware basin depocenter, its northward-thinning and syn-orogenic Wolfcamp infill, and major structures that deform the Wolfcamp including the left-lateral Grisham fault zone and Central Basin Uplift (Figure 1).

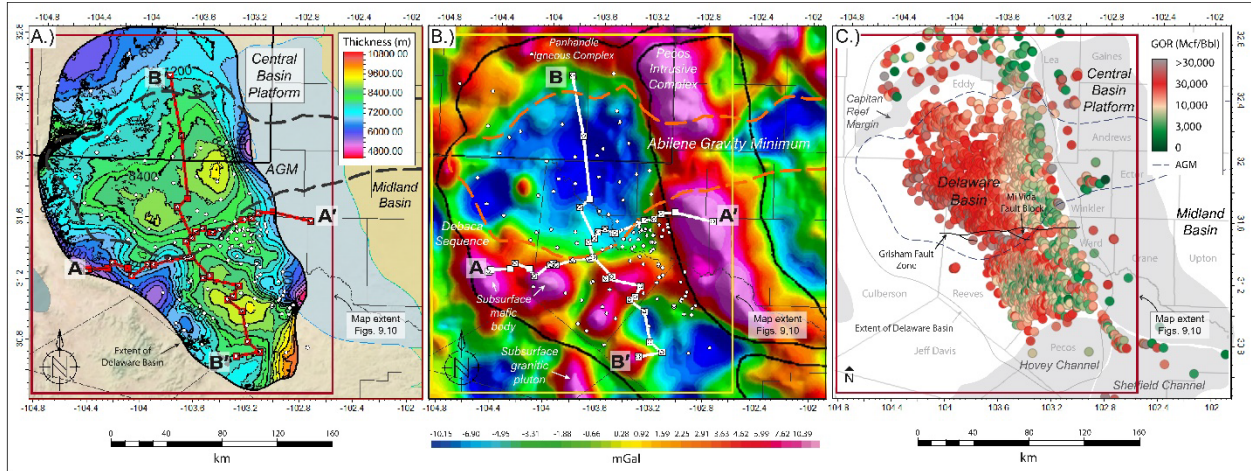


Figure 1. Location map of cross sections A-A' and B-B' over isopach map of regional sediment thickness showing basin axis oriented at roughly N34°W. (B) Location map of cross sections A-A' and B-B' over residual Bouguer gravity anomaly map of the Permian Basin study area, provided by Hualing Zhang (Zhang et al., 2021). Residual Bouguer Anomaly values are given in mGal. Subsurface mafic bodies inferred from the residual Bouguer anomaly map show more complexity than those inferred using the Bouguer anomaly. Residual Bouguer anomaly signatures suggest that the southern Delaware Basin has a higher concentration of high-density mafic basement than was previously mapped in Adams & Keller (1996). (C) Well-level, 12-month average gas-oil-ratio trend based on IHS production data for the Wolfcamp A, B, C, and D units in the Delaware Basin and surrounding areas. 12-month average GORs calculated in September 2022. GOR values are higher within the AGM. GOR values are lower south of the AGM and GFZ.

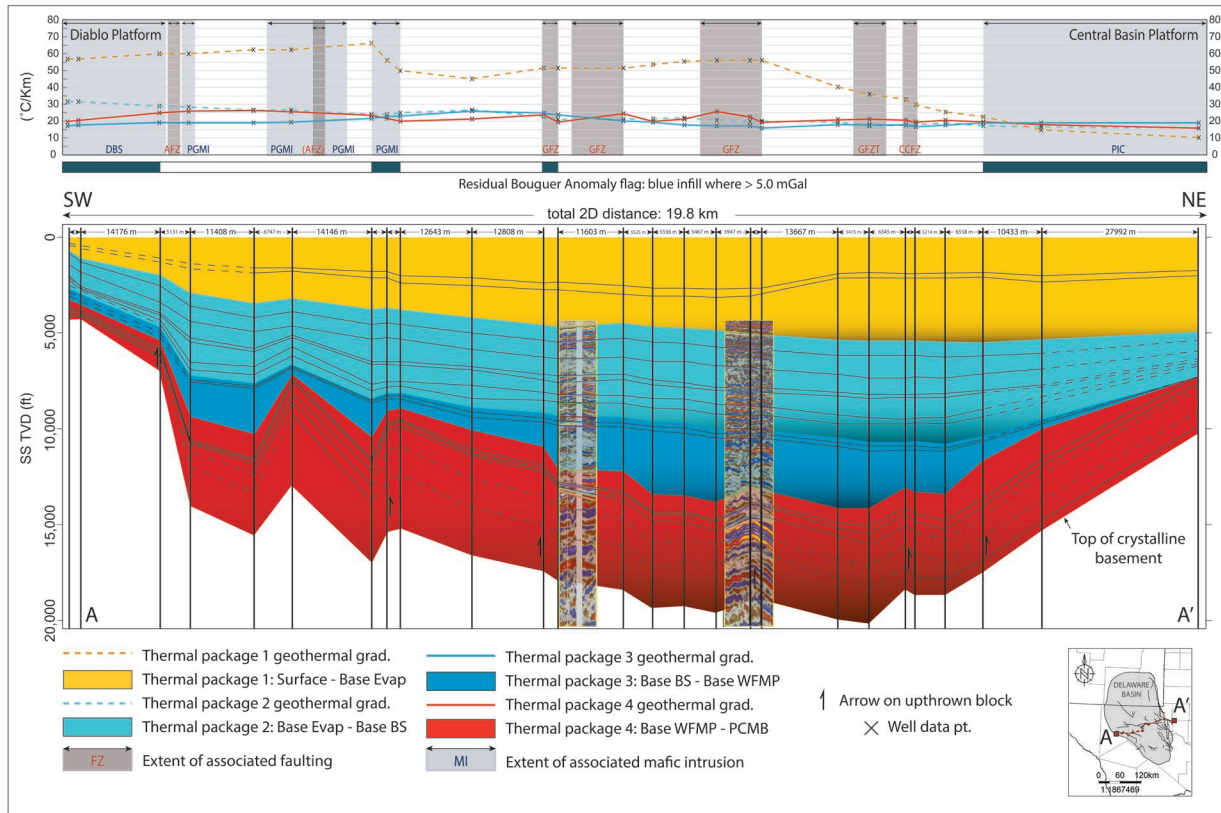


Figure 2. Southwest to northeast cross-section of the Delaware Basin showing associated interval-specific geothermal gradient histogram with residual Bouguer anomaly flag. Wells used to constrain the stratigraphic boundaries are shown as vertical black lines. Dashed correlation lines within cross-section denote interpreted stratigraphic tops from structural grids. Interval-specific geothermal gradients show strong correlation to underlying mafic bodies, faulted zones, and vertical proximity to shallow evaporite units. Fault zone and intrusive complex abbreviations are labeled according to Horne et al., (2021) and Ewing et al., (2019), respectively: DBS: De Baca Sequence, AFZ: Apache fault zone, PGMI: Pre-Grenville mafic intrusion, PIC: Pecos Intrusive Complex, GFZ: Grisham fault zone, CCFZ: Coyanosa complex fault zone.

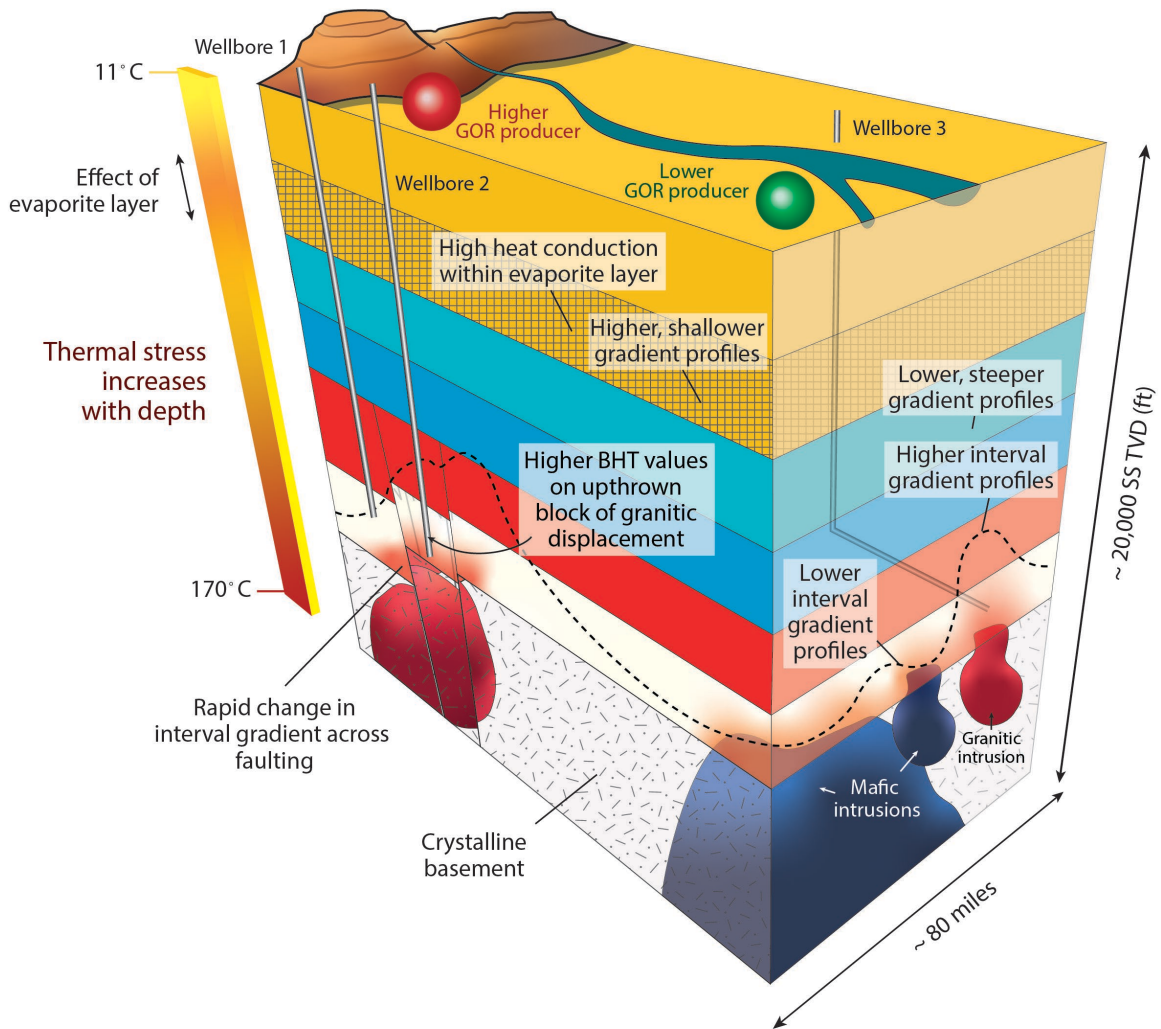


Figure 3. Conceptual diagram of sources of heat flow within the Delaware Basin showing how various subsurface lithological and structural features affect resulting heat flow, geothermal gradients, and GOR values.

6. Late Cretaceous-Recent tectonostratigraphic evolution of the Yucatan back-arc basin, northern Caribbean Sea

Juan Pablo Ramos Vargas, PhD Candidate, University of Houston

The 110,000 km² Yucatan Basin in the northern Caribbean Sea is critical for understanding the Late Cretaceous to Recent tectonic evolution of the Caribbean-North American plate boundary. This study integrates gravity, magnetic, and a 5,500 km grid of 2D seismic data to carry out a tectonostratigraphic analysis of the Yucatan Basin. These data provide the first recognition of 38–102 km-long spreading ridges that constrain a SW-NE opening direction in the western Yucatan Basin (Figure 1). The age of this oceanic crust is constrained to be late Paleocene-middle Eocene (57–42 Ma) based on heat flow measurements, depth-to-seafloor, and three sedimentary sequences inferred to be Eocene—Recent in age based on stratigraphic correlations to distant wells. We interpret the Yucatan Basin as a back-arc basin formed during the northeastward movement of the Caribbean volcanic arc that is now exposed in Cuba, evolved during the early Cretaceous to middle Eocene, and was terminated by collision with the Bahama carbonate platform during the late Paleocene to middle Eocene (Figure 1). We identify regional, left-lateral strike-slip faults that extend into the Cuban volcanic arc, as observed in other active back-arc basins. We propose that the Yucatan back-arc basin once formed the northwestern extension of age-equivalent back-arc basins in Hispaniola, where the basin is inverted, topographically elevated, and strongly shortened, and in the Lesser Antilles where the Paleogene back-arc basin has remained undeformed and submarine. This once-continuous back-arc basin was disrupted and left-laterally offset by ~500 km during the Late Eocene-Recent formation of the Cayman trough strike-slip system.

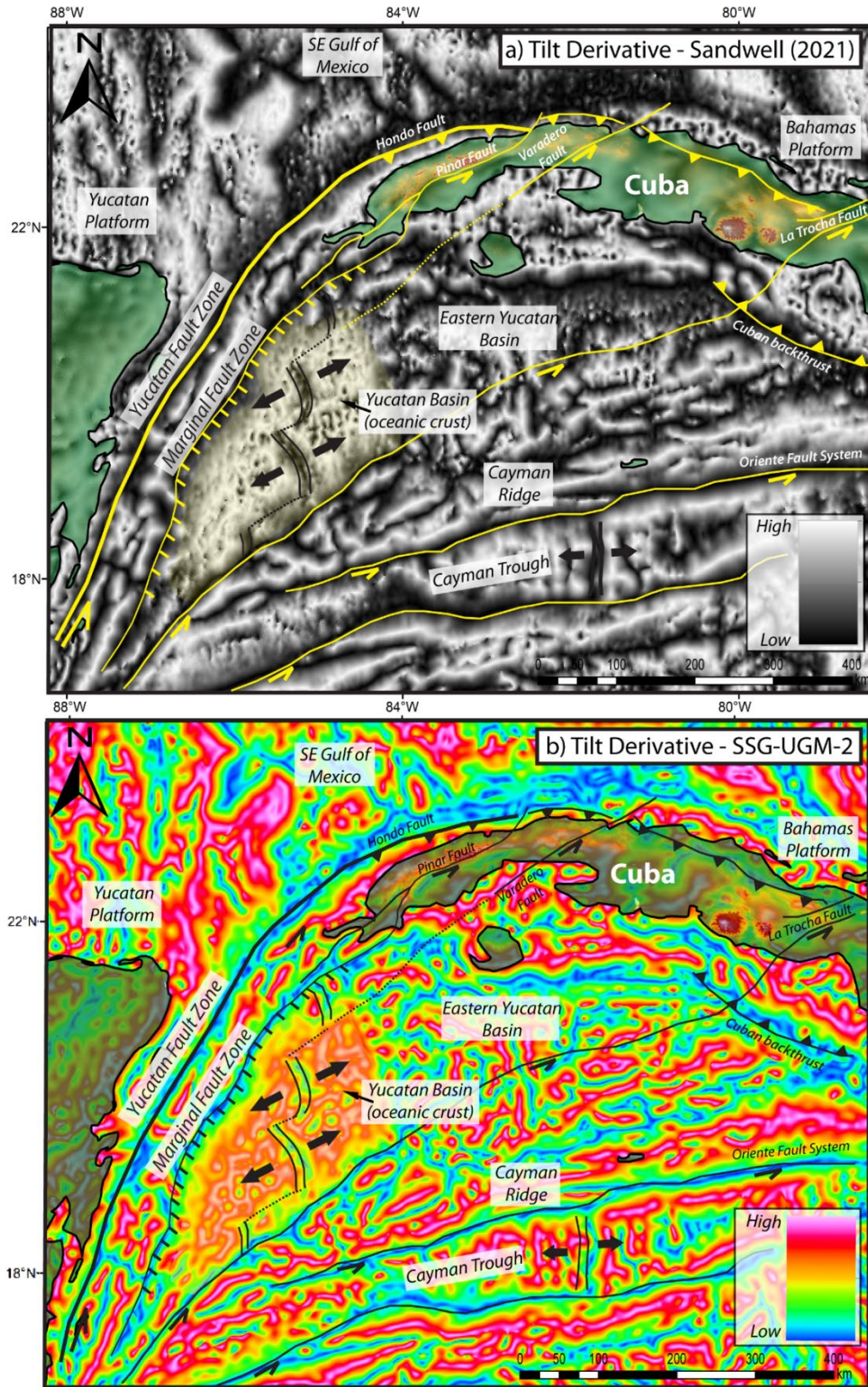


Figure 1. A) Tilt-angle (TA) gravity filter was applied to the marine satellite gravity data from Sandwell et al. (2014) to reveal the area of oceanic crust formed along short spreading ridges in the western part of the Yucatan back-arc basin along with the northeast-striking and left-lateral strike-slip faults

shown in yellow that extend across the in the Yucatan back-arc basin and into the Cuba-Bahamas arc-continent collisional zone. B) Tilt-angle (TA) gravity filter was applied to the SGG-UGM-2 marine satellite gravity data from Liang et al. (2020) showing details of the same features seen in A. Black arrows show the change in opening direction from the northeast direction the in the late Paleocene-Middle Eocene Yucatan back-arc basin to the more east-west direction in the Cayman trough. This change in the direction of Caribbean plate motion was the result of the terminal collision of the Cuban arc with the Bahamas platform and the reorientation of the Caribbean Plate into a more eastwardly direction.

7. Crustal structure of the Bahamas platform and implications for basin modeling

Kenneth Shipper, PhD Candidate, University of Houston

The 14,000 km² wide Bahamas carbonate platform has largely impeded knowledge of the underlying crustal structure and type due to the reduced seismic reflection penetration depth, lack of recent reflection or refraction surveys, and limited deeply penetrating wells. Without this data, the effects of the Triassic-Jurassic Central Atlantic opening and Middle Eocene Cuban orogeny are unknown (Figure 1). These primary effects include: 1) Contribution of radiogenic heat production of the crust to potential source rocks; 2) Transient basal heat flow variation as a function of uplift and erosion during the Cuban orogeny; and 3) Comparisons of the continent-oceanic-transition (COT) to the Guyana-Suriname and Guinea-Mauritania margins. This study aims to alleviate these uncertainties and study their primary effects by integrating all publicly available seismic reflection and refraction data, filling in gaps of missing data with forward modeling using free-air gravity data, inverting the Moho along 9 2D regional transects, modeling the flexural uplift of the crust with the resulting basement and gravity data, then testing RHP values for several 1D basin models constrained by downhole temperatures (Figure 2).

The resulting crustal structure constrained by 409 regional refraction controls and 56 local refraction controls along the 9 transects indicates a variation of crustal thickness from 27-10 km with a rugose thinning of 6 km from northwest to southeast (Figure 1). Elastic thickness variations from the flexural modeling indicate a similar trend with 18-23 km thick elastic crust thinning to 12-20 km from northwest to southeast. Flexural uplift varies from 2 km near the western Florida Straits to a high of 6 km offshore northwest Hispaniola. Temperature controls from the Cay Sal-1, Doubloon Saxon-1, and Great Isaac-1 wells were used to calculate RHP of the resulting modeled crust. Due to the uncertainty of lithospheric thickness near the Cuban suture zone, a range of 205-179 km was applied to Doubloon-Saxon-1 and Cay-Sal-1. The resulting RHP varies from 1.5 mW/m³- 1.25 mW/m³ at Cay Sal-1 and .24 mW/m³ - 0 mW/m³ at Doubloon Saxon-1 for 205-179 km lithosphere. Great Isaac-1 exhibited a constant lithospheric thickness of 100 km and resulted in .45 mW/m³.

Based on the modeled crustal structure, RHP variation, and presence of salt diapirism at the Exuma Sound basin, we interpret three crustal domains: 1) 27-12 km thick thinned continental crust just southeast of Exuma Sound to the Blake Plateau with 18-23 km thick elastic crust and 1.37-.19 mW/m³ decreasing RHP to the southeast; 2) 24-12 km thick volcanically thickened oceanic crust on the Bahamas hotspot 90 km southeast of Long Island with 12-15 km thick elastic crust; 3) 20-12 km thick volcanically thickened oceanic crust offshore northern Hispaniola with 20 km thick elastic crust (Figure 2).

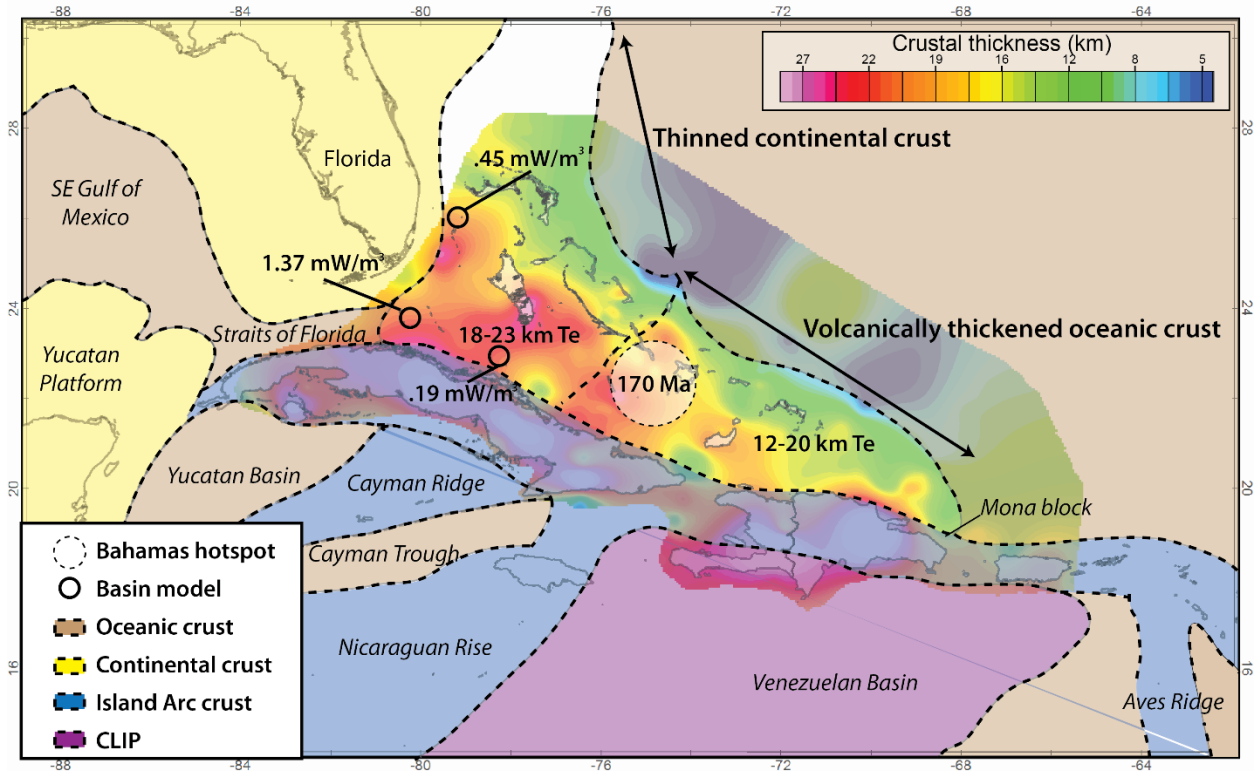


Figure 1. Standard thermal stress (STS) map at the Santonian source interval based on constant radiogenic heat production (RHP) per unit thickness of continental crust within the Guyana-Suriname basin. RHP from the oceanic crust is assumed to be zero (Allen and Allen, 2013). The map on the top right indicates 3D basin model size and compares STS to overburden thickness of the Maastrichtian-present interval. STS values are compared to known oil and gas fields as indicated by the green and red polygons. The extent of Cretaceous and Tertiary turbidite systems is indicated by the dashed and dotted lines, respectively (Ballard, 2019).

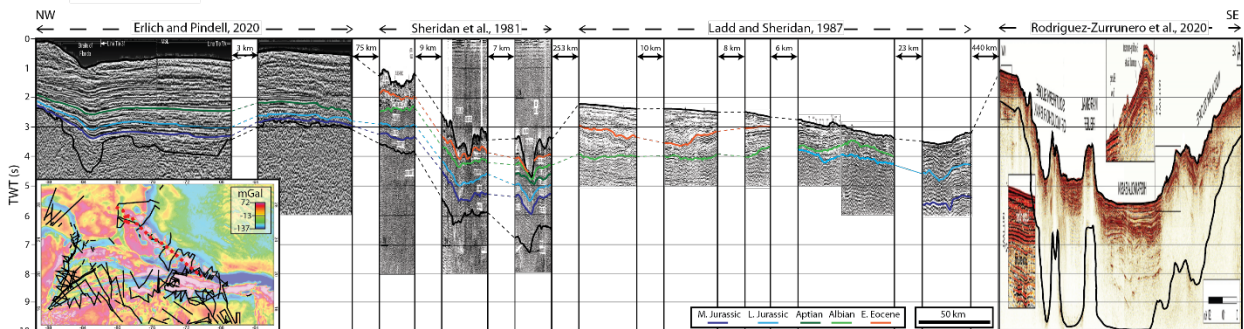


Figure 2. Total crustal thickness derived from basement and Moho topography interpolated from gravity models of transects A-I. Interpreted crustal domains from NW-SE are shown by thin black lines. Reconstructed hotspot is indicated by the dashed circle. Large igneous plateau crust of the Bahamas and southeastern North America are shown with thick black lines to correlate with low elastic thickness (T_e). RHP (radiogenic heat production) values in the thinned continental crust of NW Bahamas are shown at 1D model locations represented as thick circles.

8. Basin modeling of the Eocene to Present forearc San Pedro Basin (Dominican Republic offshore)

José Miguel Gorosabel Araus, Research Associate 1, University of Houston

Paul Mann, CBTH Project Principal Investigator, Professor of Geology, University of Houston

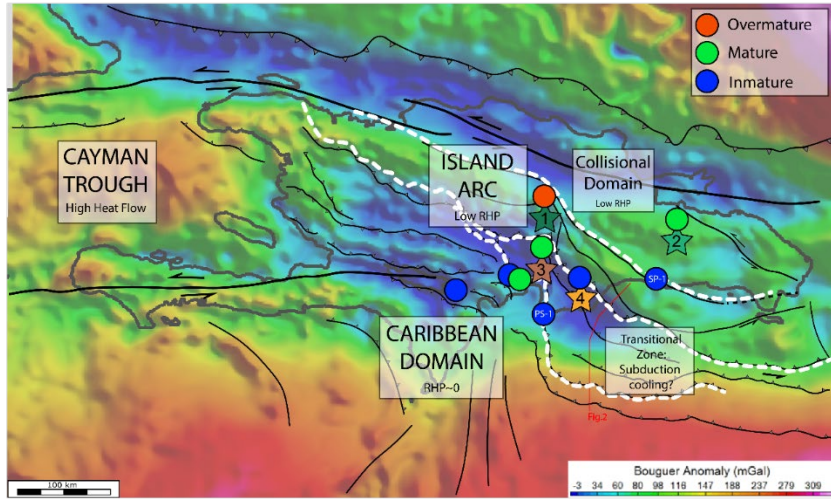
Jose-Luis Granja-Bruña, Professor, Complutense University of Madrid

The Dominican Republic has a limited history of oil production, with only about 50,000 barrels produced in the 1940s from the Azua Basin. This oil was primarily attributed to Middle Miocene carbonate source rocks and reservoirs within the Upper Miocene/Lower Pliocene turbiditic sandstone. As a result, hydrocarbon exploration over the subsequent decades has mainly targeted the Miocene and younger rock formations.

This study presents recent results showing the potential for source rocks in Upper Cretaceous, Eocene, and Oligocene clastic rocks based on field sampling in the eastern and central Dominican Republic (Figure 1). We analyzed up to 80 potential source rock samples from outcrops, of which 42 underwent analysis for Total Organic Carbon (TOC), while 16 were subject to Rock-Eval with studies of their biostratigraphic age and sedimentary facies. In order to improve offshore correlations to the offshore San Pedro basin, we analyzed 60 onshore and coastal wells and re-processed legacy seismic profiles provided by the Dominican National Hydrocarbon Dataset (Banco Nacional de Datos de Hidrocarburos, BNDH), along with seismic profiles, gravity, and magnetic data from several Spanish marine surveys. These data allow improved well-to-outcrop-to-seismic reflection line correlations and improved post-mortem analysis of dry holes in the area, leading to the interpretation of the main elements of the petroleum system in the offshore SPB (Figure 2).

Our analyses have identified three potential source rocks dating to the Cretaceous, Eocene, and Oligocene periods and the previously recognized Miocene source in the Azua production area. TOC values in these rocks ranged up to 3.6%Wt for Cretaceous, 0.98% for Eocene, and 0.95% for Oligocene formations. Regionally, kerogen types displayed variations tied to their geologic age. While Cretaceous samples oscillated between type II (oil-prone) and type III (gas-prone), Paleogene samples predominantly showcased type III kerogen, underscoring their gas-prone nature. Oligocene to lower Miocene carbonate and clastic rocks show fair to good porosities and permeabilities in onshore wells. Structural and stratigraphic traps formed since the Oligocene–Middle Miocene are considered in this study as the primary objective. However, trap preservation is an exploration risk due to the ongoing tectonic activity in the area.

This information has been integrated with regional geothermal, structural, and tectonic data to complete the basin modeling for the offshore SPB. The SPB region shows a low heat flow and thermal conductivity, leading to an expected geothermal gradient of between 20 – 25 °C/km. Although our results point out the hypothetical oil generation for the Cretaceous section, the main exploration risk is represented by the presence of this interval in the basin, with the middle-upper Miocene being the critical point of the system. We attribute this low heat flow to the nature of the granitoid of the arc and the interaction of the dual subduction on the mantle convection.



- Potential source rocks sampled for this work:
- ★ Conician - Santonian. TOC: from 0.78 to 2.7 %Wt
 - ★ Middle Eocene. TOC: up to 0.98 %Wt
 - ★ Cenomanian? - Santonian?. TOC: up to 0.56 %Wt
 - ★ Oligocene. TOC: up to 0.95 %Wt

Figure 1. Interpretation of the main structural domains overlaid on the Bouguer anomaly map. Stars indicate the locations of source rock samples. Circles represent locations with thermal data, which includes wells and outcrops.

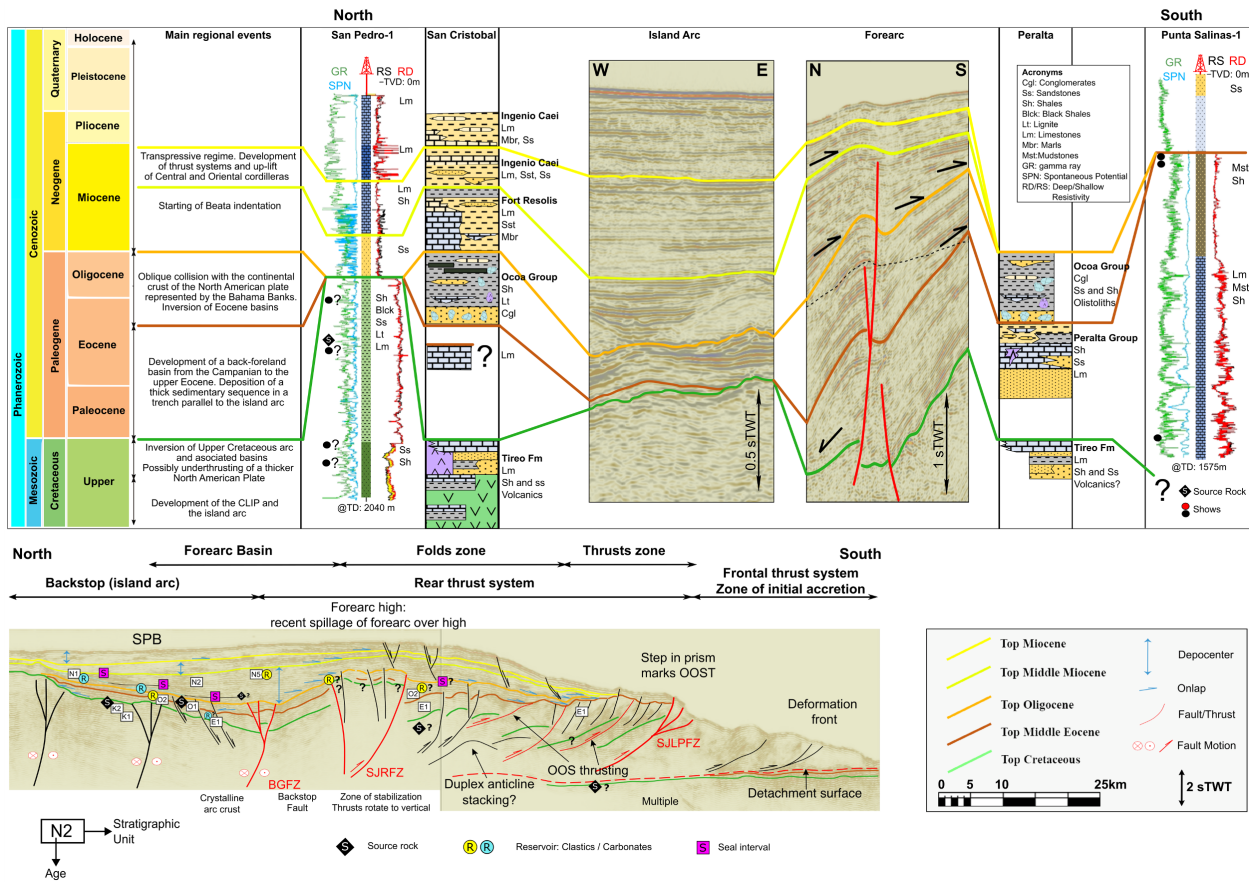


Figure 2. Above, onshore-offshore correlation of geological and geophysical data for the San Pedro Basin. Below, the interpretation provided in this study for seismic line SD-5, see location in Figure 1.

SOUTH AMERICA

- Chapter 9 - Crustal structure in the Colombian Basin and its control on the distribution of potential source rock and play fairways in deep and ultra-deep waters of the Caribbean by Juan Pablo Ramos Vargas
- Chapter 10 - Control of crustal thickness, type, and burial history on heat flow and petroleum basin modeling of the Guyana-Suriname rifted-passive margin by Kenneth Shipper
- Chapter 11 - The Barreirinhas Basin: An unexplored frontier with significant potential in the Brazilian Equatorial Margin by José Miguel Gorosabel Araus, Paul Mann, Alanny Melo, David Castro, and Diógenes C. Oliveira
- Chapter 12 - Syn-rift and salt depositional thicknesses in the rift zones of the Espirito Santo-Campos-Santos salt basin, Brazil, as a result of the southwestward tilting of the basement by Sharon Cornelius
- Chapter 13 - Exploring the external kitchen of the Campos Basin, Offshore Brazil using cutting-edge 3D seismic data by Ruth Beltran
- Chapter 14 - Transferring deepwater play concepts from hydrocarbon discoveries in Namibia to its conjugate margin in Argentina by Daniel Maya

9. Crustal structure in the Colombian Basin and its control on the distribution of potential source rock and play fairways in deep and ultra-deep waters of the Caribbean

Juan Pablo Ramos Vargas, PhD Candidate, University of Houston

We integrate 8,210 km of 2D seismic data, 13,200 km² of 3D seismic data, the compilation, and integration of published information from scientific (DSDP/ODP) along with publicly-available hydrocarbon exploratory wells, seafloor samples, oil seeps, geochemical evaluations, and potential field methods. The seismic data used for this project includes some of the most recently acquired and processed seismic reflection data in the Colombian Basin and the Northern Panama Deformed Belt (NPDB). Interpretations from potential gravimetric and magnetometry methods were also carried out to assess the basement architecture and the location of the main depocenters, and tectonic features in the region. Seismic interpretation integrated with potential field data shows that the basement underlying ultra-deep waters of the Colombian Basin includes a zone of 5-7 km normal-thickness oceanic crust with a SW-NE trending spreading ridge (Figure 1). We infer that the sedimentary fill of these rough oceanic crust controls potential Late Cretaceous age source rocks time-equivalent to organic-rich rocks recovered by DSDP drilling on three sites located >80 km away from this area. The upper part of the sedimentary sequence has different seismic facies interpreted as turbidites and deep-water deposits associated with the development of the Magdalena Fan since the Miocene, as well as MTCs of Pleistocene age. This thick accumulation of the Miocene to recent Magdalena deep-sea fan provides widespread, stacked, and high-quality reservoirs, seals, and overburden to late Cretaceous source rocks. This thick, Miocene-to-recent Magdalena fan section exhibits numerous amplitude anomalies that are consistent with 4-way structures with more than 8 km of length located mainly trending along the toe of the slope (Figure 2). We also show results from the separate Northern Panama Deformed Belt to the west that shows semi-continuous Bottom Simulating Reflectors (BSRs) as well as similar 4-way structures as seen in the Colombian waters.

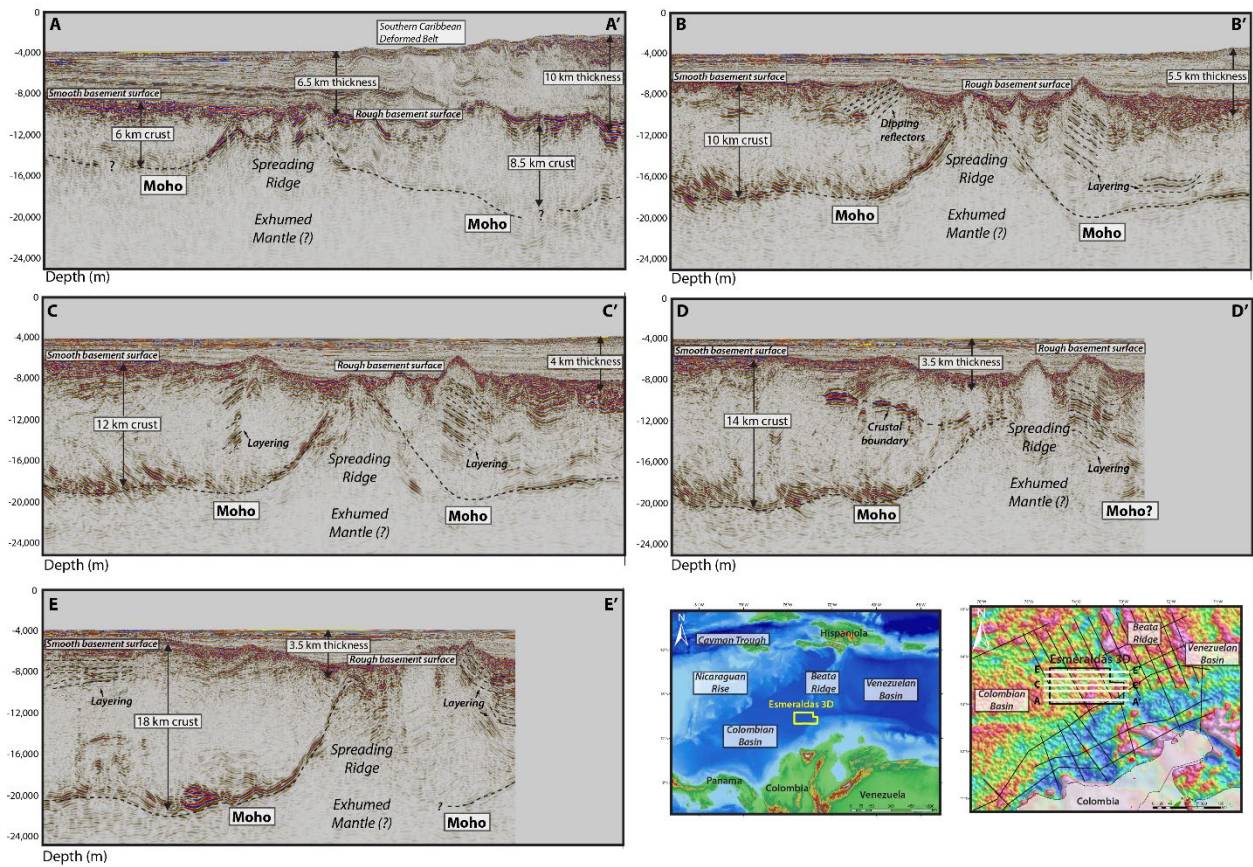


Figure 1. Interpretation of five east-to-west lines (inline) from the Esmeraldas 3D seismic survey in deep waters of the Colombian basin that move from south (A-A') to north (E-E'). The interpretations show how variations in basement type and thickness control the sedimentary thicknesses in this part of the Colombian Basin. A) The southern transect exhibits a normal oceanic crust between 6-8 km thick with a spreading ridge in the center of the figure. The sedimentary thickness along this transect is >6 km and reaches >10 km in the Southern Caribbean Deformed Belt. B) Moving north, transect B-B' shows how the crust thickens northward to more than 10 km in the northwestern survey area. C) Moving northward this transect shows the extinct spreading center in the center of the line that is characterized by an abrupt shallowing in the Moho and the presence of a rough basement surface with an axial valley containing a greater thickness of sedimentary infill. D) The interpretation shows that the thickened crust (>14 km) west and east of the spreading ridges has a clear layering as well as dipping reflectors likely associated with volcanic eruptions. E) The change from thick oceanic crust (>18 km) in the west to thin and very-thin oceanic crust (<3 km) in the east influences sedimentary thickness with areas of thin oceanic crust having a thicker sedimentary cover while the areas of thickened crust and smooth basement surface have a thinner cover. F) First-vertical-derivative gravity map at the location of the 3D survey in the Colombian Basin which shows the location of the five transects shown in A-E and their gravity response. The age of the thin oceanic crust observed in all the cross-sections is unknown since no exploratory wells have sampled it. We interpret the upper part of the thickened crust as part of the Caribbean Large Igneous Province (CLIP) of Late Cretaceous age drilled in the DSDP wells in the central Caribbean located 80 km from the location of the 3D survey.

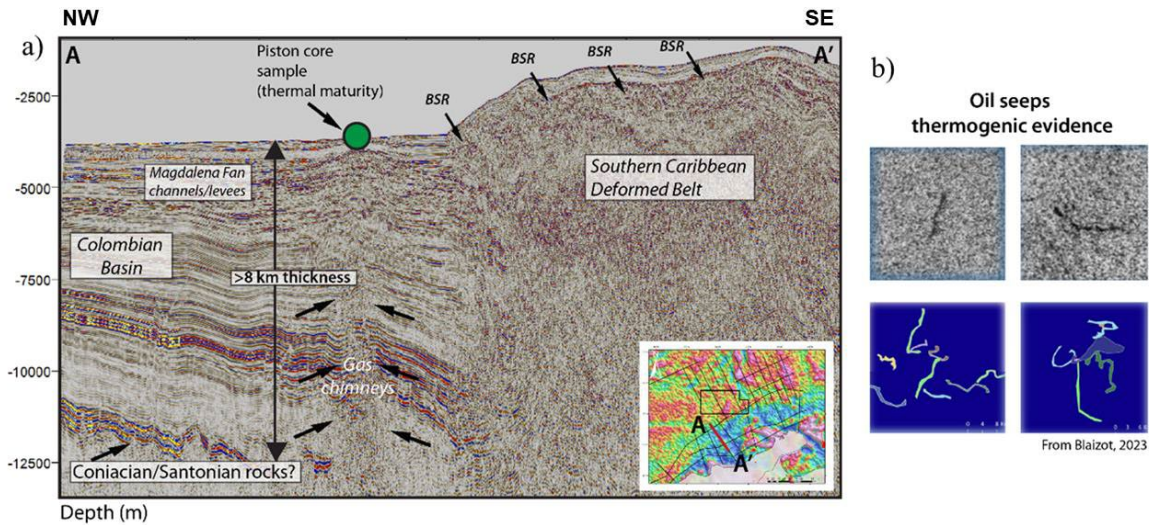


Figure 2. A) Cross section of the Colombian Basin which shows the location of a piston core sample based on an interpretation by Ramirez et al. (2015) for thermal maturity based on the presence of diamondoids and biomarkers recovered from the piston core from the area of seeps shown in B. The seismic line in A shows the location of the seep area on the seafloor directly overlies an inferred gas chimney that arises from the deepest part of the sedimentary section in this area of the Colombian basin. These deeper parts of the sedimentary section exhibit high-amplitude, low-frequency horizons interpreted as potential Coniacian/Santonian rocks which have been proven to have an excellent potential for hydrocarbon generation from the intervals recovered from the DSDP wells (Carvajal-Arenas et al., 2020). B) Besides the thermogenic evidence reported based on the seafloor samples, recent analyses in the Colombian Basin have shown the presence of oil seeps in the region from high coverage SAR Satellite images which were shared with me by Clement Blaizot in February of 2023 for this research. These different pieces of evidence support the idea of an untapped thermogenic petroleum system that has not been explored in the deep waters of the Colombian Basin. This research seeks to correlate and provide further analysis between variables such as crustal type, sedimentary thickness, heat-flow values, and the presence of this potential petroleum system in order to guide future exploratory activities in the region.

10. Control of crustal thickness, type, and burial history on heat flow and petroleum basin modeling of the Guyana-Suriname rifted-passive margin

Kenneth Shipper, PhD Candidate, University of Houston

Crustal type (granitic/basaltic) and thickness are vital to determine the variability of thermal stress beneath rifted passive margins. The resulting variations in thermal stress also control petroleum generation and prospectivity, and therefore understanding thermal stress can be used to predict petroleum fairways. We integrate crustal thickness structure and radiogenic heat production (RHP) from the Guyana-Suriname margin to construct full lithosphere thermal transient models that can be extended along the entire margin to predict variations in thermal stress and source rock maturity.

The crustal structure in the non-volcanic area of the Guyana basin provided by our 3D gravity inversion indicates a highly-tapered rifted profile that thins from a pre-rift thickness of 40-50 km in the Guiana cratonic shield to a rifted thickness of 6-8 km across a 170-km-wide necking zone. In the southeastward along-strike direction, the non-volcanic Guyana margin transitions to the Demerara volcanic margin over an along-strike distance of 282 km and is locally characterized by thick, 25-km-thick seaward dipping reflectors. The Demerara volcanic margin in Suriname formed as the expression of a late Jurassic (197-173 Ma) plume head and hotspot track coeval with the rifted crustal structure as seen on the non-volcanic Guyana margin. This study interprets seven stratigraphic horizons across the 43,680 km² Stabroek block using a grid of 2D KPSTM seismic reflection lines. This study integrates previously published lithofacies, uncorrected downhole temperatures, and vitrinite reflectance measurements.

We integrate the interpreted horizons, well stratigraphy, temperature data, crustal structure, paleowater depth, and timing of tectonic phases to calibrate RHP to predict the lateral variations in the thermal history of source rocks on the Guyana-Suriname margin using the ExCaliber modeling software from Xplorlab (Figure 1). Based on this understanding of the crustal architecture of the non-volcanic Guyana margin and the volcanic Suriname margin, we use five wells across both areas to define three crustal domains: 1) 10-30-km-thick continental crust with ~46-12 mW/m² RHP with absent or minor volcanic rocks adjacent to the continent-ocean boundary; 2) 15-km-thick continental crust with ~16 mW/m² RHP with thick, overlying SDRs that are more landward from the COB; and 3) 6-8-km-thick oceanic crust with zero RHP in the deep, oceanic area of the Guyana basin. Using average geothermal gradient as a relative indicator, the gradient at 5 km depth below mudline changes from 24.1 °C/km above oceanic crust to 30.5 °C/km along Guyana's non-volcanic margin while the gradient of the volcanic Demerara margin increases with underlying granitic crustal thickness from 25 °C/km to 29 °C/km. The continental contribution of heat flow compared to oceanic contribution proportionally varies from 46 mW/m² to 0 mW/m² RHP.

The presence of thin continental crust beneath the volcanic margin and shallower source rocks combine to delay the timing for oil expulsion from Late Cretaceous to Pleistocene as a result of the decreasing thermal stress from the diminishing RHP. Transient thermal effects above cold oceanic crust related to 1.9 km of Miocene to recent clastic sedimentation results in oil expulsion during the Pleistocene.

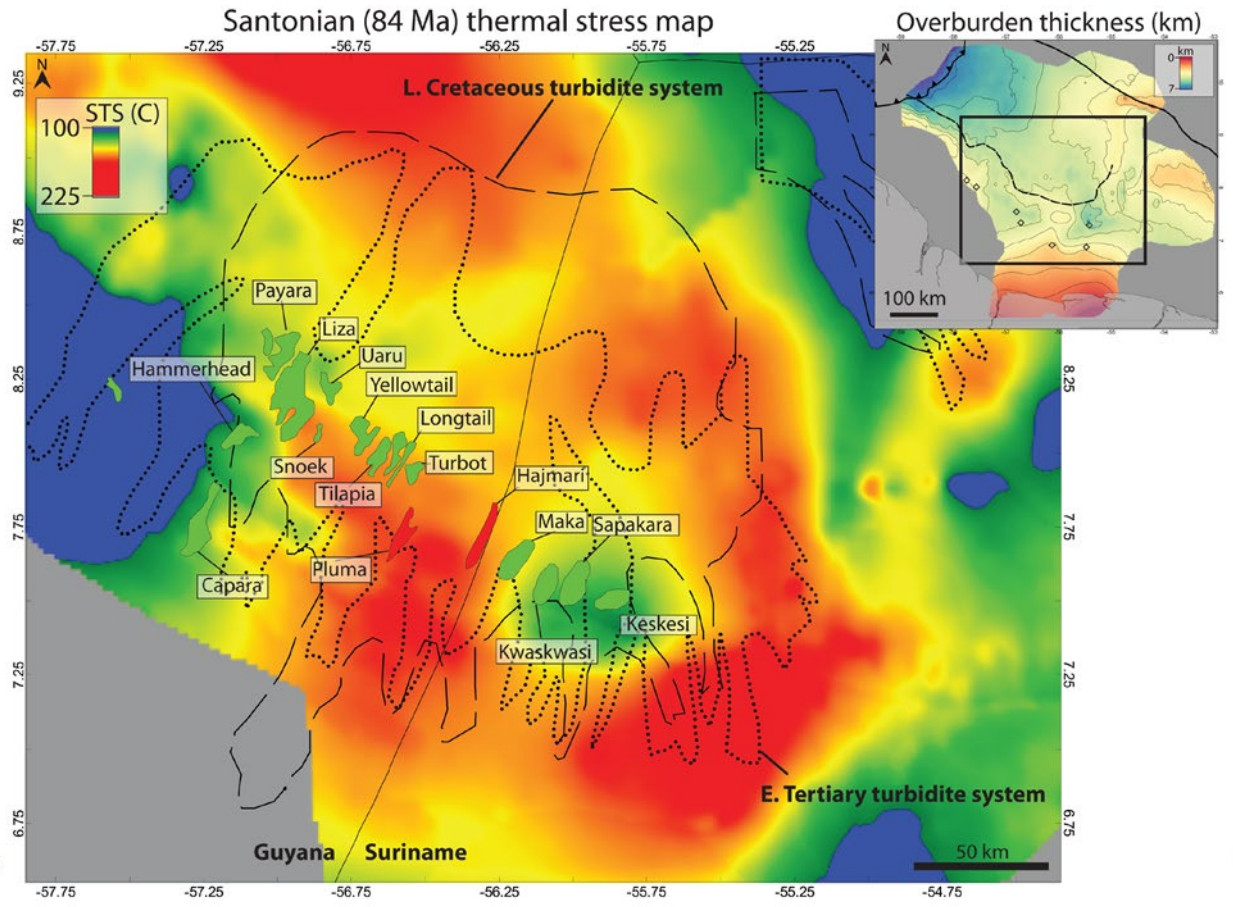


Figure 1. Compilation of published 2D seismic lines along the central NW-SE Bahamas carbonate platform. Connection between seismic lines is indicated by the dashed red line on the free-air gravity (Liang et al., 2020) map on the bottom left. Interpretations are modified from (Erlich & Pindell, 2020; Sheridan et al., 1981; Ladd & Sheridan, 1987; Rodriguez-Zurrunero et al., 2020). Note lack of penetration to basement and scarce seismic throughout central Bahamas.

11. The Barreirinhas Basin: An unexplored frontier with significant potential in the Brazilian equatorial margin

José Miguel Gorosabel Araus, Research Associate 1, University of Houston

Paul Mann, CBTH Project Principal Investigator, Professor of Geology, University of Houston

Alanny Melo, Post-Doctoral Researcher, Universidade Federal do Rio Grande do Norte

David Castro, Professor, Universidade Federal do Rio Grande do Norte

Diógenes C. Oliveira, Professor, Universidade Federal do Rio Grande do Norte

The Barreirinhas Basin, located along the Brazilian equatorial margin, attracted the attention of exploration companies following significant discoveries in its conjugate margin in Ghana, such as the Jubilee oil field. However, despite this initial interest, the basin remains largely unexplored. Exploration activity has been focused on the shelf, targeting plays associated with the main rifts in the proximal and necking domains. Only 3 of the 18 wells drilled were in the external area in deep waters, highlighting the untapped potential of the distal and marginal rifts of the basin.

This research aims to determine the true prospectivity of the Barreirinhas Basin, with a particular emphasis on the most external rifts and their relationship with their African conjugate.

The Barreirinhas basin is located at the western end of the Romanche Fracture Zone (Figure 1). It is one of the basins configuring the Brazilian Equatorial Margin, along with the Foz do Amazonas, Maranhao, Ceara, and Potiguar basins. These basins are related to the Early Cretaceous (Aptian-Albian) opening of the Equatorial Atlantic. This margin, classified as a transform to oblique-rifted margin, is characterized by a narrow necking zone with a steep transition from a thick continental crust (~30 km) to a highly thinned region (<10 km). In the case of the Barreirinhas basin, this thinning is constrained to a narrow zone of only 12 km, resulting in a pronounced slope along the passive margin, leading to gravitational compressive systems (Figure 2).

The hydrocarbon prospectivity of the Barreirinhas Basin is further enhanced by the discoveries in its African conjugate, the Tano Basin off Ghana. A prime example is the Jubilee field, which produces oil from Turonian source rocks, coupled with Upper Cretaceous reservoirs and seals. Samples from the Barreirinhas Basin and its surrounding areas have also revealed the presence of potential source rocks for the period Albian-Turonian, which suggests that the Barreirinhas Basin may also potentially host oil and gas reserves.

In collaboration with the Universidade do Rio Grande do Norte in Brazil, our interdisciplinary research aims to de-risk exploration in the basin by identifying the main oil and gas kitchens. To do this, we have interpreted seismic data and integrated it with well data, gravity and magnetic data, gravity and structural models, geothermal information, and geochemical characterization of source rocks to complete the basin modeling. Through this, we seek to understand the relationship between heat flow and the complex crustal structure of the basin.

Preliminary results indicate the presence of potential source rocks in the basin for the period Albian-Turonian, which may have reached the generation window. Potential plays are also complemented by the Coniacian-Campanian turbidite system interpreted on seismic lines. These plays will be assessed by completing a comprehensive 2D mapped basin modeling for the main potential source rocks.

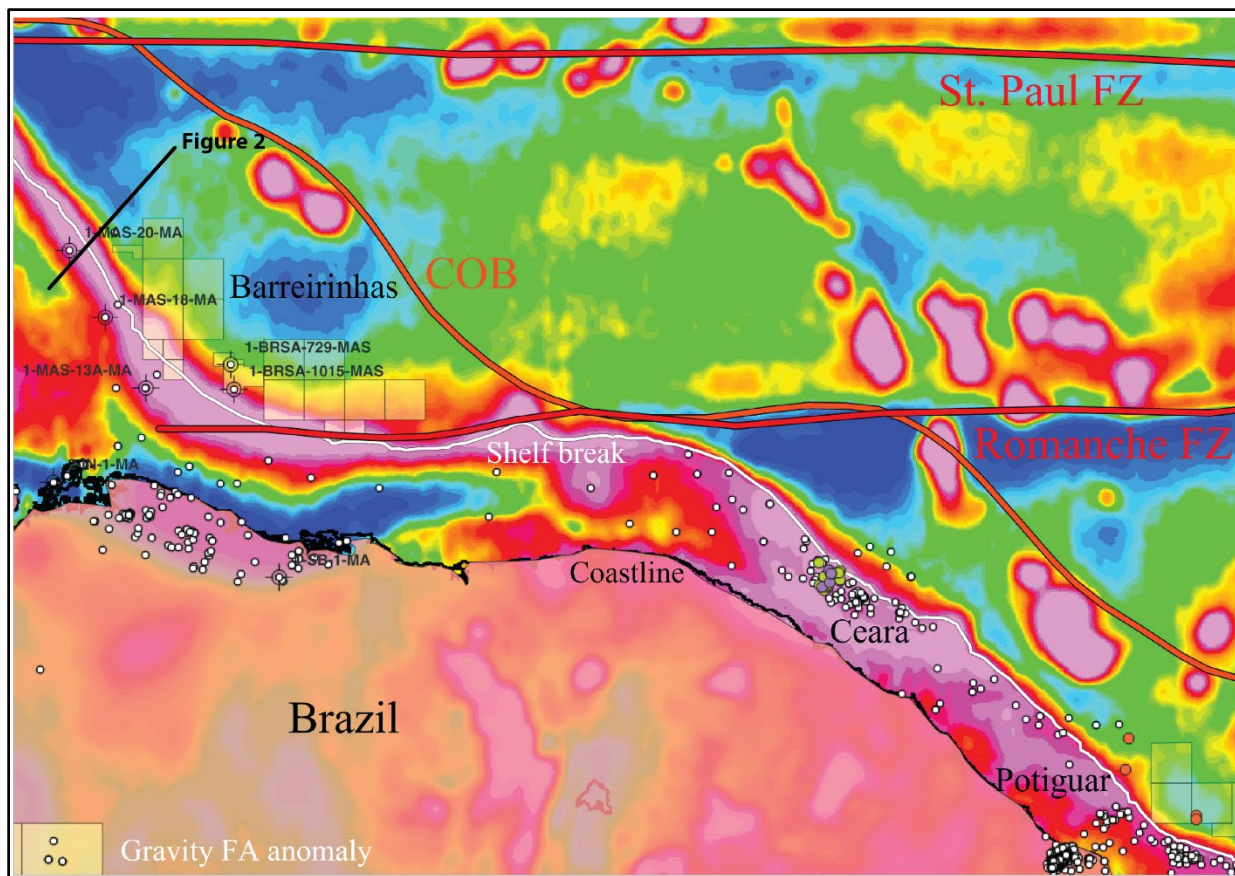


Figure 1. Free air anomaly map of the Barreirinhas, Ceara, and Potiguar Basins, showing the main structural features and previous wells.

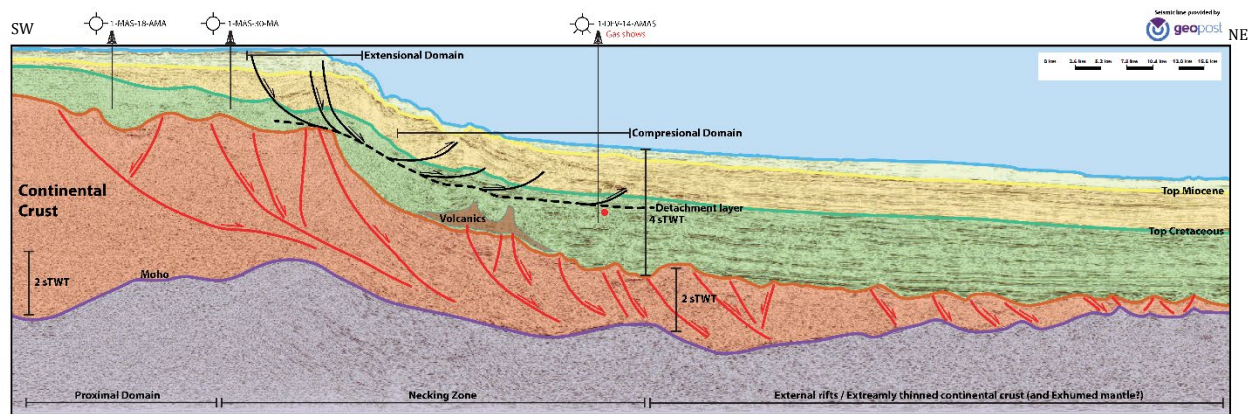


Figure 2. Interpretation given in this study for a representative seismic section of the Barreirinhas Basin.

12. Syn-rift and salt depositional thicknesses in the rift zones of the Santos-Campos-Espirito Santo salt basin, Brazil, resulting from the southwestward tilting of the basement

Sharon Cornelius, Research Associate 2, University of Houston

Current research efforts are directed towards estimating the external rift zone viability in terms of hydrocarbon potential east of the external high, along which most of the current subsalt production exists for these three connected Brazilian basins. A reasonable basin model that will point out areas of likely oil and gas accumulations, as well as areas of both thermal immaturity and over-maturity, requires the following surfaces: 1) depth to the seafloor; 2) depth to the top of salt; 3) depth to the base of salt; 4) depth to the top of basement rocks; and 5) depth to the top of the Moho surface. As a result, the following isopachs were created: 1) thickness of post-salt sediments; 2) thickness of salt; 3) thickness of syn-rift sediments composed of both source and reservoir rocks; and 5) thickness of continental and oceanic crusts.

The Moho surface was mapped using all 30 of the Ion Brazil Span seismic lines that image down to 40 km and cover these three salt basins. The depth to the top of the crystalline basement was mapped for all three basins three times using three different basin-wide seismic data sets provided by TGS. All seismic data used were depth-migrated either by pre-stack depth migration (PSDM) or by reverse-time migration (RTM). The first data set was very dense in coverage (~120,000-line km) but did not cover the southeastern part of Santos. The second data set was less dense in coverage (only ~30,000-line km) but did have the advantage of imaging more of southeastern Santos. This second data set shown in Figure 1 did show a tilt from NE to SW because some data points were >16 km deep. This second basement surface map showed the top of continental crust drops 3900 m over a map distance of 978 km in the external rift zone, and the top of oceanic crust drops 3100 m over a map distance of 1160 km from NW to SW. To preserve the detail of the first map and still be able to image the whole of Santos, the Brazil Span seismic data lines for these basins were incorporated into the workstation project of the first data set to give greater detail above 16 km depth but to also delineate any deeper basement data points (Figure 1).

Due to the localized thickness of source and reservoir rocks, and the salt in the rift zones, the implication is that this basement tilt may have existed at the time of initial rifting (~132Ma) for the first rift attempt that was between the shoreline and the external high (the Merluza Graben area), resulting in the prolific hydrocarbon source rocks (Type 1 kerogen) of the “internal kitchen”. These source rocks are from lacustrine shales. This southwestward tilt was present during the main rifting event (~112 Ma) that was outside the external high, resulting in the inconclusive hydrocarbon province known as the “external kitchen” (Figure 1). Eleven wells drilled thus far outboard the designated pre-salt zone have shown two dry holes, one oil well, five gas wells, and three oil plus gas wells. These recent gas discoveries open two possible explanations: the source rock of the external rift may have a marine component, or the geothermal heat flux may be greater in the external rift zone.

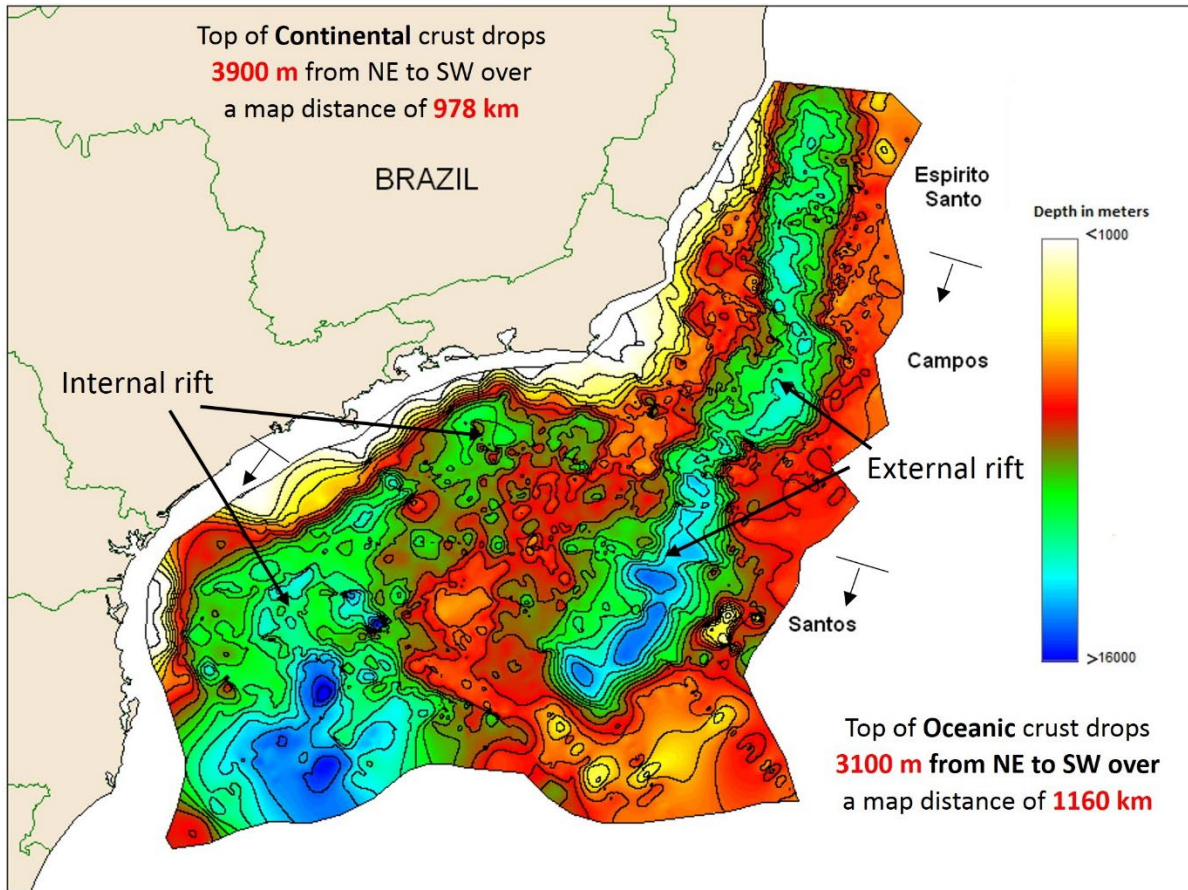


Figure 1. The regional depth to basement map shows both the internal and external rift zones separated by the external high (in red) between the two rifts. Measurements were taken in the external rift zone for continental crust and outside the C-O-B for the oceanic crust.

13. Exploring the external kitchen of the Campos basin, Offshore Brazil using cutting-edge 3D seismic data

Ruth Beltran, PhD Candidate, University of Houston

The Campos Basin is located along the southeastern Brazilian margin and was created by the Early Cretaceous rifting of continental crust between South America and West Africa. Two complex and margin-parallel rift systems occupy the tapered zone of thinned, continental crust that underlies the passive margin section of the Campos basin: one rift system underlies the slope, and the other rift underlies the ultra-deepwater area directly adjacent to the continent-ocean boundary that is marked by zone of exhumed mantle (Figure 1). This study aims to establish the presence of a key source-reservoir interval in the deepwater area of the Campos basin, Brazil, and helps to de-risk exploration in this area.

This study integrates potential fields, refraction seismic data, and deep-penetration seismic reflection data from the Campos-Santos basin to illustrate the locations of the sub-parallel Internal kitchen (Merluza rift) in a more landward location and the External kitchen in the deepwater area adjacent to the oceanic crust which forms the focus of this study (Figure 1). Within our 68,000 km² study area of the External kitchen we use 20,000 km of 2D seismic lines and 3D seismic data to image the upper Barremian Coquinas unit.

Seismic data shows the Coquinas Formation thickens from 100 m at the edges of the rift to 500 m within the rift. Reflectors can be seen onlapping the rift highs and are consistent with these rocks being deposited in a lacustrine setting (Figure 2). In addition, four main stratigraphic surfaces have been mapped based on constraints from well data: 1) Moho at the base of a necked zone of 10-22 km thick continental crust that underlies the External kitchen; 2) pre-rift early Barremian; and 3) late Aptian unconformity (base of salt). As a result, a set of structural and isopach maps with these surfaces was created to illustrate the External kitchen evolution during the Aptian (Figure 2).

Regional maps of gravity using various filters illustrate the NE-trending Internal kitchen (Merluza rift) which is the more landward and (Aptian) rift system that terminates at a narrowing and failed rift tip in the southwestern Campos basin (Figure 1). In comparison with the Merluza rift, the External rift exhibits NNE trend, a more uniform, and less tapered width, and is more discontinuous with three prominent gravity lows along its trend (Figure 1). The gravity maps and deep seismic data indicate the crustal structure thinning from 22 km to 10 km across the hyperextended crust zone along the Campos margin. This External kitchen area is bounded by a gravity high to the west and the continent-ocean boundary to the east forming a rift in ultra-thin continental crust (Figure 1).

Future work will be focused on an inversion modeling of gravity and magnetic data, restoration of seismic sections, and mapping more horizons in the overburden section to have more control for basin modeling.

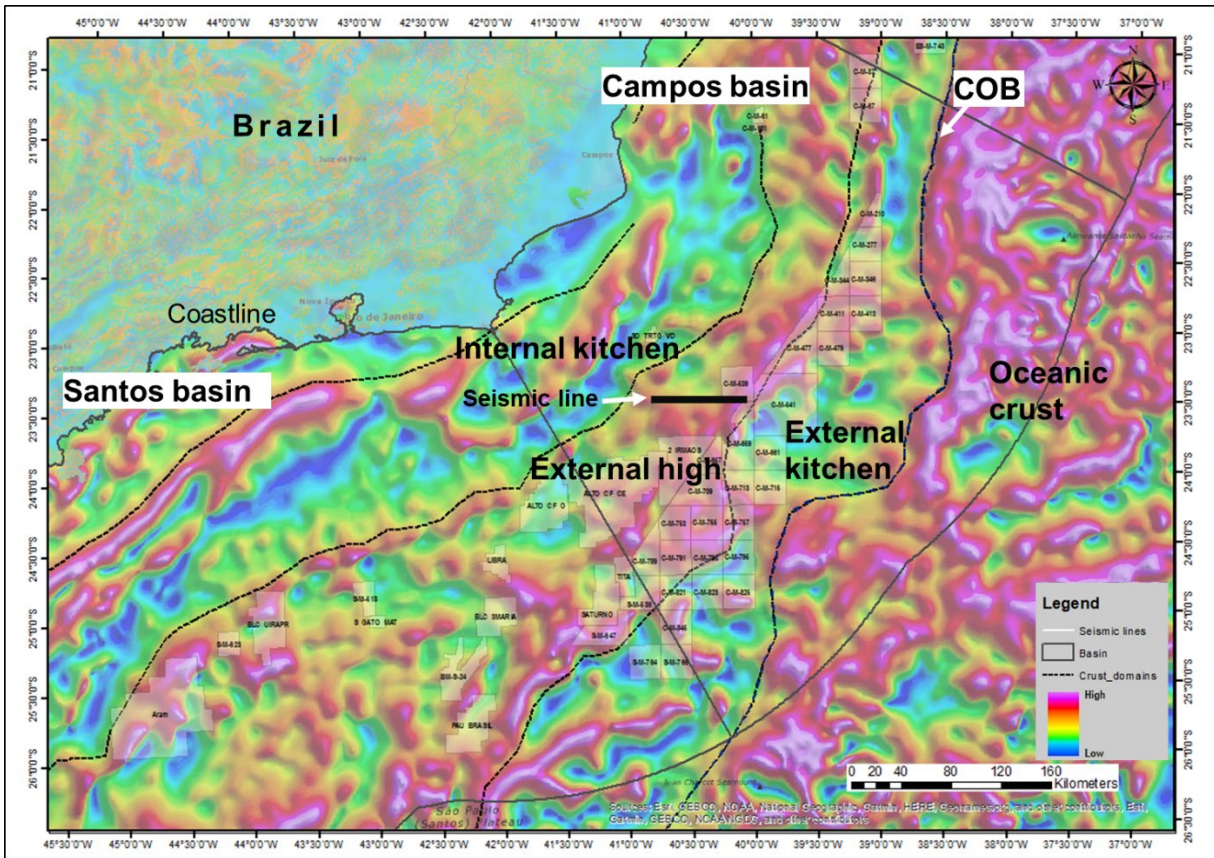


Figure 1. Tilt derivative gravity map showing the sub-parallel Internal kitchen (Merluza rift) and the more seaward External kitchen including three depocenters. These rifts had migrated oceanward within the upper Barremian and Aptian time range. The dashed black line outlines the External High in the Santos and Campos basins, a positive structure considered a regional focus for oil migration.

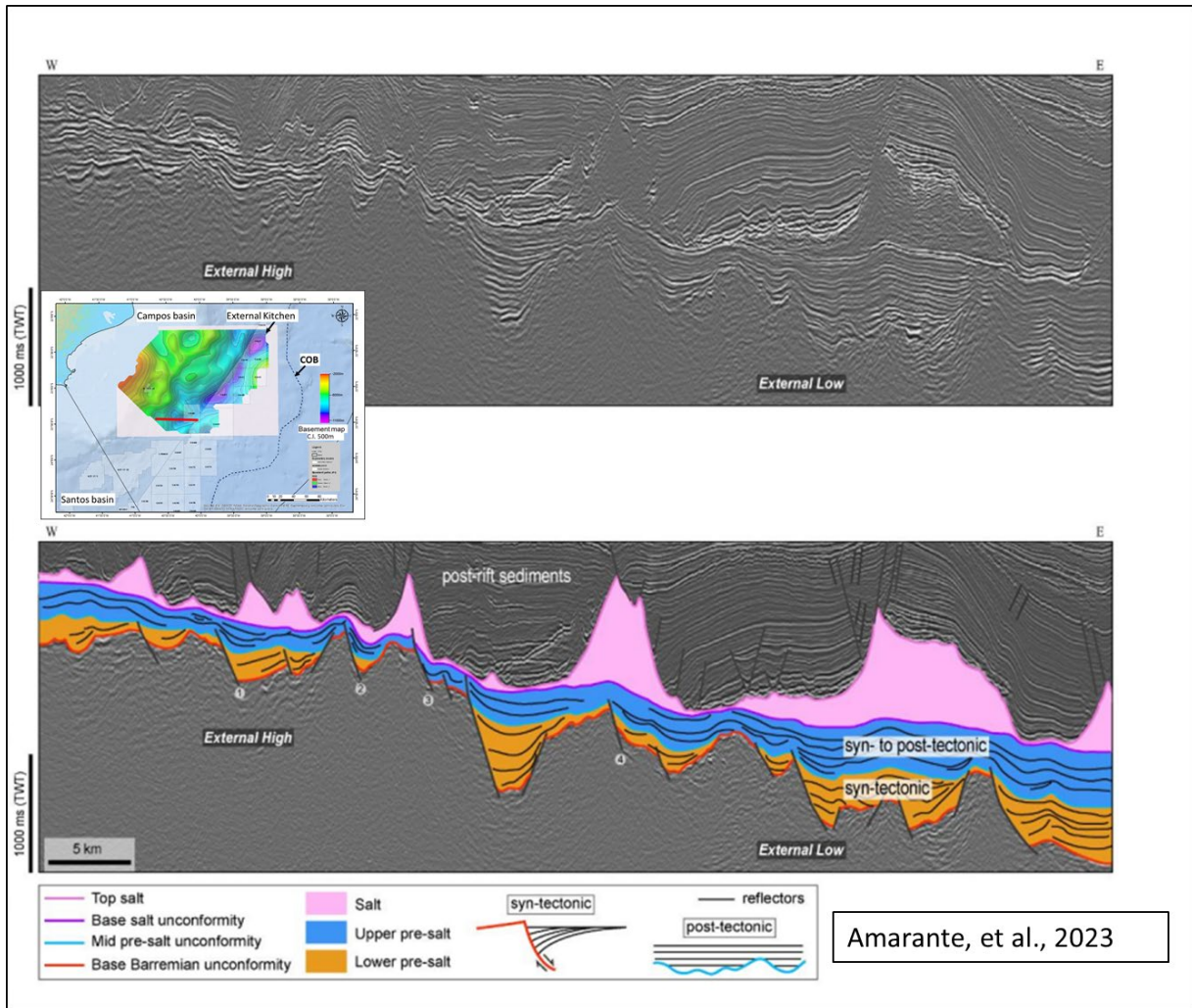


Figure 2. An uninterpreted and interpreted seismic line from Amarante et al. (2023) that displays the stratigraphic surfaces discussed in this research.

14. Transferring deepwater play concepts from hydrocarbon discoveries in Namibia to its conjugate margin in Argentina

Daniel Maya, PhD Candidate, University of Houston

Northern Argentina and Southern Namibia share similarities as conjugate rifted-passive margins with volcanic origins formed during the late Jurassic and early Cretaceous periods. These margins exhibit 2-13 km-thick volcanic units that filled initial rifts, resulting in plateau-like formations upon which passive margins developed.

In Namibia, the volcanic-rifted margin features an Outer High ridge characterized by basaltic, seaward-dipping reflectors known as SDRs (Figure 1). This ridge divides the passive margin basinal sediments into an inner sub-basin formed during the Neocomian and an outer sub-basin that developed later during the Aptian when this part of the margin submerged into abyssal water depths. Notably, in Namibia's deep-water Venus and Graff oil discoveries, totaling 11 BBOE, the seismic evidence reveals the presence of a secondary reservoir covering the majority of the Outer high with 100 m thickness in the 4.2-4.3 km range along the Outer High ridge and clastic reservoirs as the main one spanning the 4.8-5.3 km intervals within submarine channel systems, overlaying the carbonate reservoirs.

The northern Argentinean margin and its Namibian counterpart share a significant tectonic feature. This Outer High ridge is the same as the demarcation zone between the inner and outer sub-basin. The inner sub-basin, situated within the northern Argentinean offshore area, has witnessed extensive exploration efforts, marked by the drilling of 26 non-commercial exploration wells on the continental shelf. These drilling endeavors have spanned depths ranging from 5 to 88 meters as explorers sought out Permian and Late Jurassic-Early Cretaceous plays. While these plays have been identified, they have proven to be non-prolific. The failed rifts in this zone helped us understand the tectonic history and petroleum systems before the Gondwana breakup.

In contrast, the outer sub-basin, constituting the deep-water margin, has remained a largely unexplored zone. Compelling geological parallels with the Namibian deep-water region come to light, particularly concerning the presence of the same highly productive Aptian source rock characterized by marine shale. This shared geological foundation raises the possibility of a promising deep-water petroleum system. Seismic analysis further reinforces this potential, revealing total organic carbon (TOC) levels exceeding 3%-4%. Along the expanse of the Outer High Ridge, one encounters the presence of carbonate rock-type reservoirs, which extend up to 200 meters in thickness. Additionally, the eastern flank of the Outer High, along with the slope and basin floor, hosts clastic reservoirs formed by turbidite fans, boasting a thickness of 1.3 kilometers (Figure 2).

Furthermore, the Aptian source rock in the Colorado basin is buried beneath ~3500 meters of sediments. Meanwhile, the Aptian source rock in the Salado Basin is buried beneath ~5100 meters (Figure 2), with a considerable average thickness measuring ~384 meters. These striking geological similarities collectively suggest the feasibility of hydrocarbon stratigraphic trapping and a possible up-dip migration through the slope, paving the way for a promising future in petroleum exploration.

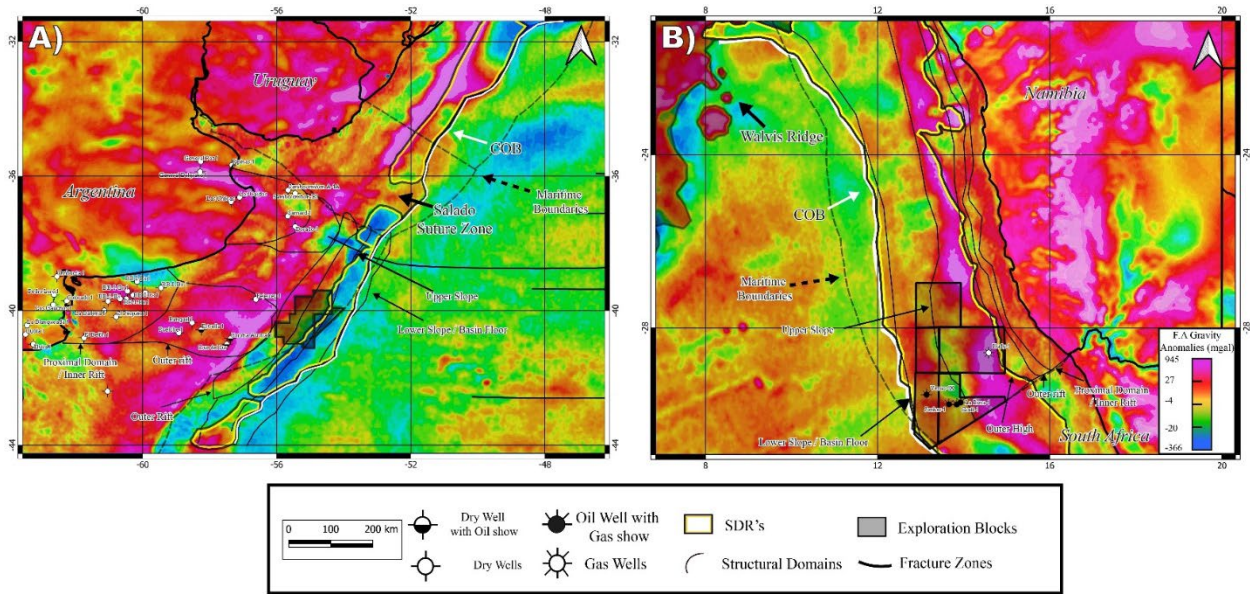


Figure 1. A) Free-air anomaly map of the Northern Argentinean margin shows thin black lines showing the main structural domains. The white line represents the COB. The polygon with an outer black line and an inner yellow line represents the SDRs (Seaward Deeping Reflectors). The gray polygons represent the main exploration block in Argentinean deep water where drilling plans exist for testing the deep-water petroleum system. The cut line represents the maritime boundaries between Argentina and Uruguay. B) A free-air anomaly map of the Namibian margin shows the thin black lines showing the main structural domains. The white line represents the COB. The polygon with an outer black line and an inner yellow line represents the SDRs (Seaward Deeping Reflectors). The gray polygons represent the main exploration blocks in the Namibian deep water. The cut line represents the maritime boundaries between Namibia and South Africa.

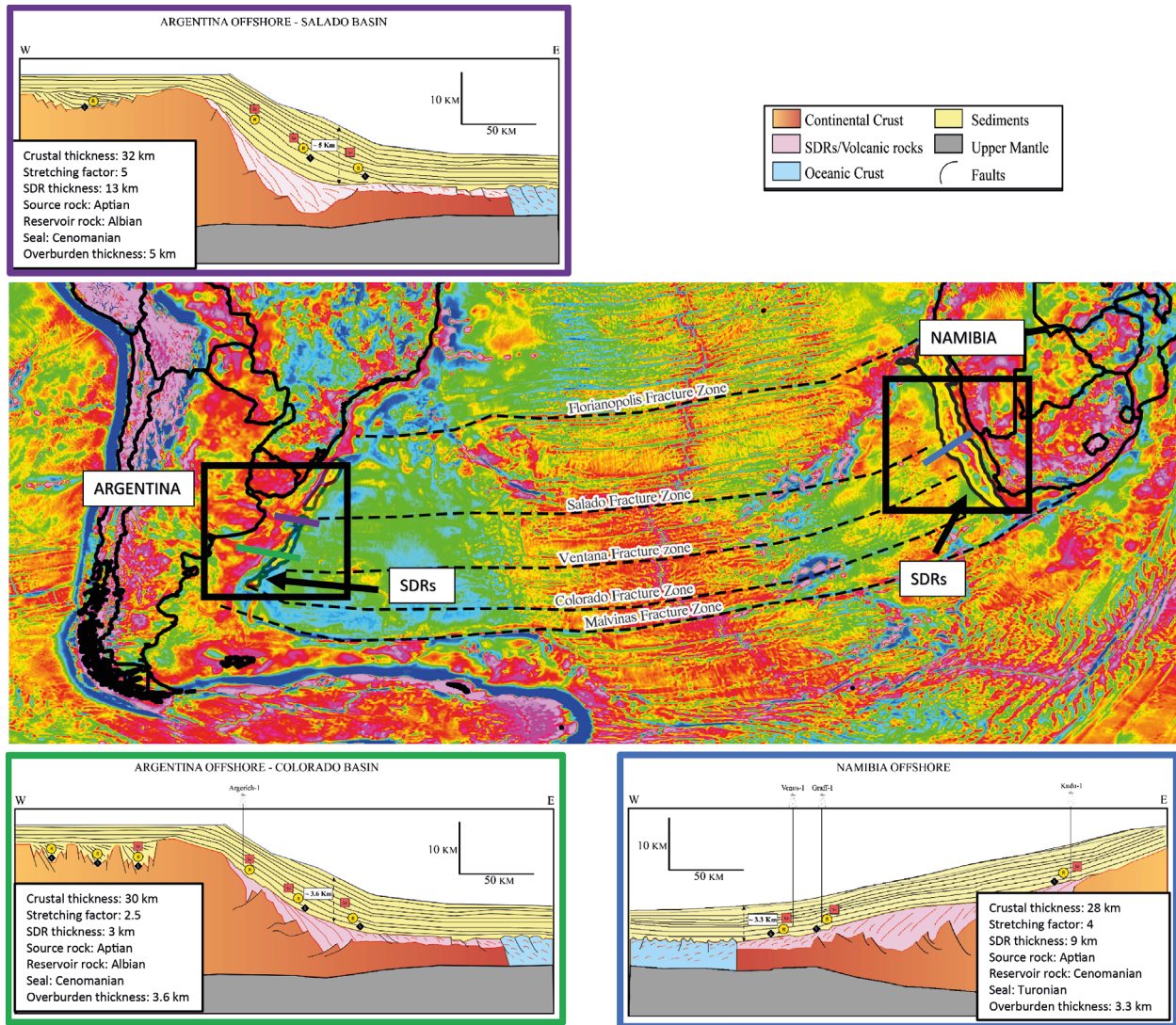


Figure 2. Free air anomaly map showing the conjugate margin of Namibia and Argentina with three different schemes. Purple cross section based on Pollitt and Sun (2023), Reuber et al. (2019), and Turrini et al. (2017) in the Salado and Punta del Este Basin. The green and blue cross sections are based on DeVito and Kearns (2022), Chauvet et al. (2021), Reuber et al. (2019), and Dressel et al. (2017). Those schemes show the crustal thickness, stretching factor, and SDRs thickness. The black diamond shows the source rock, the yellow circle represents the reservoirs, and the orange squares represent the seals.

WEST AFRICA

- Chapter 15 – Tectonic controls on Mesozoic source rock thermal maturity of the 3500-km-long, rifted-passive Atlantic margin of Morocco by Paul Mann, Md Nahidul Hasan, and Tarek Galhom
- Chapter 16 – Crustal structure and hydrocarbon potential of the non-volcanic and volcanic, rifted-passive margins of Mauritania by Md Upal Shahriar
- Chapter 17 – Hydrocarbon prospectivity of deeply-buried Early Cretaceous rifts of the western deepwater area of the Niger delta, Nigeria by Jumoke Akinpelu
- Chapter 18 – 3D and 2D mapping and basin modeling of the Rio Muni Basin by José Miguel Gorosabel Araus
- Chapter 19 – Relationships between Red Sea opening directions, crustal types and thicknesses, evaporite distribution, and hydrocarbon potential by Mohamed Abdelfatah

15. Tectonic controls on Mesozoic source rock thermal maturity of the 3500-km-long, rifted-passive Atlantic margin of Morocco

Paul Mann, CBTH Project Principal Investigator, Professor of Geology, University of Houston

Md Nahidul Hasan, PhD Graduate, University of Houston (now at BP)

Tarek Galhom, MS Graduate, University of Houston (now at University of Bergen)

The rifted-passive margin of Morocco with the Central Atlantic Ocean extends 3500 km from the Strait of Gibraltar to the northern border of Mauritania and forms the conjugate margin for much of the eastern USA and maritime Canada. All areas of the Moroccan margin are experiencing a slow but steady, oblique convergence between the African and Iberian continental plates that has produced widespread basin inversions, plateau uplifts, infrequent but large oblique-slip earthquakes like the 2023 Morocco earthquake and the 1755 Lisbon earthquake, and broad folding of the oceanic crust of the Central Atlantic Ocean. This convergence began in the Late Cretaceous due to the opening of the South Atlantic Ocean. Convergent effects become more pronounced in northern Morocco and southern Iberia (Figure 1).

In the first part of this study, we interpret a grid of ~8474 line-km of pre-stack, depth-migrated, 2D seismic reflection profiles, publicly-available gravity and well data, and 2D gravity models from the Atlas Mountain termination to the Strait of Gibraltar (Figure 2, 3). Gravity modeling and seismic interpretation reveal a ~750 km elongate, 50-80-km-wide marginal rift that forms a basement low overlying a zone of rifted continental crust. The marginal rift parallels the modern coastline of Morocco and crosscuts the east-northeast orogenic and Mesozoic rift grain of northwestern Africa. Calibrations of downhole temperature measurements from the Tantan-1 and DSDP-416 offshore wells were used to constrain 1D and map-based thermal maturity models to quantify the hydrocarbon potential of source rocks ranging in age from Triassic to Late Cretaceous. Calibration of downhole temperature measurements from the Tantan-1 within the thinned continental crust of the marginal rift and the DSDP-416 wells on the oceanic crust of the Central Atlantic shows that the geothermal gradient in the marginal rift is 29 °C/km and the gradient in the oceanic crust is 23 °C/km. However, variation is possible due to a low number of calibration wells. Modeling shows that the absence of radiogenic heat in the oceanic crust results in relatively lower geothermal gradients and can explain the immaturity to the early oil window of source rocks in these deepwater areas. Deeply-buried Triassic and Jurassic source rocks are mature for petroleum generation along the southern ~400 km-long segment of the marginal rift as validated by a compilation of the locations of previous offshore producing wells and shows. Late Cretaceous - Base Cenozoic uplift and margin erosion were observed as a major angular unconformity and break in vitrinite reflectance from wells in the offshore area. The absence of Early Cretaceous deltaic deposits in the northern 350-km-long segment of the northern marginal rift explains why Cretaceous source rocks have remained immature in this area of less sedimentary overburden (Figure 3).

In the second part of the study, we interpret a grid of ~8474 line-km of pre-stack, depth-migrated, 2D seismic reflection profiles, publicly-available gravity and well data, and 2D gravity models from the Tarfaya-Dakhla margin of southern Morocco (Figure 4, 5). Gravity modeling and seismic interpretation reveal a ~750 km elongate, 50-80-km-wide marginal rift that forms a basement low overlying a zone of rifted continental crust. The marginal rift parallels the modern coastline of Morocco and crosscuts the east-northeast orogenic and Mesozoic rift grain of northwestern Africa. Calibrations of downhole temperature measurements from the Tantan-1 and

DSDP-416 offshore wells were used to constrain 1D and map-based thermal maturity models to quantify the hydrocarbon potential of source rocks ranging in age from Triassic to Late Cretaceous. Calibration of downhole temperature measurements from the Tantan-1 within the thinned, continental crust of the marginal rift and the DSDP-416 wells on the oceanic crust of the Central Atlantic shows that the geothermal gradient in the marginal rift is 29 °C/km and the gradient in the oceanic crust is 23 °C/km. However, variation is possible due to a low number of calibration wells. Modeling shows that the absence of radiogenic heat in the oceanic crust results in relatively lower geothermal gradients and can explain the immaturity of the early oil window of source rocks in these deepwater areas (Figure 5). Deeply-buried Triassic and Jurassic source rocks are mature for petroleum generation along the southern ~400 km-long segment of the marginal rift as validated by a compilation of the locations of previous offshore producing wells and shows. Late Cretaceous - Base Cenozoic uplift and margin erosion were observed as a major angular unconformity and break in vitrinite reflectance from wells in the offshore area. The absence of Early Cretaceous deltaic deposits in the northern 350-km-long segment of the northern marginal rift explains why Cretaceous source rocks have remained immature in this area of less sedimentary overburden.

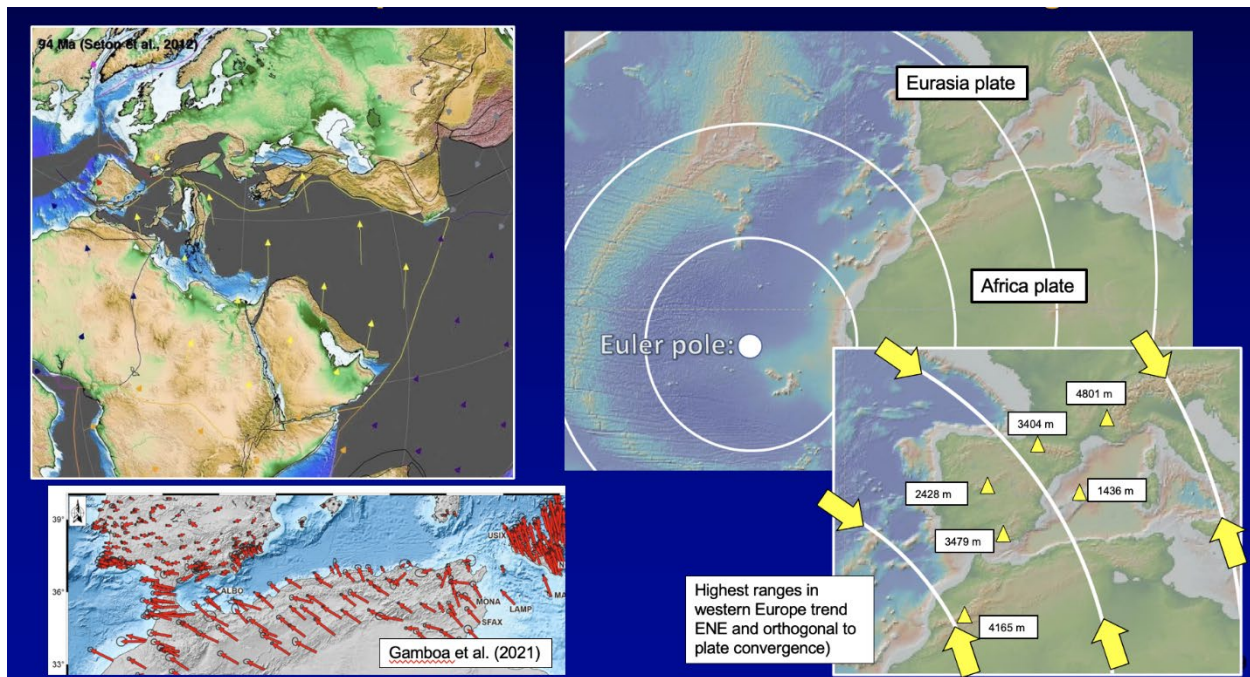


Figure 1. Regional maps from previous studies showing convergence in the study area.

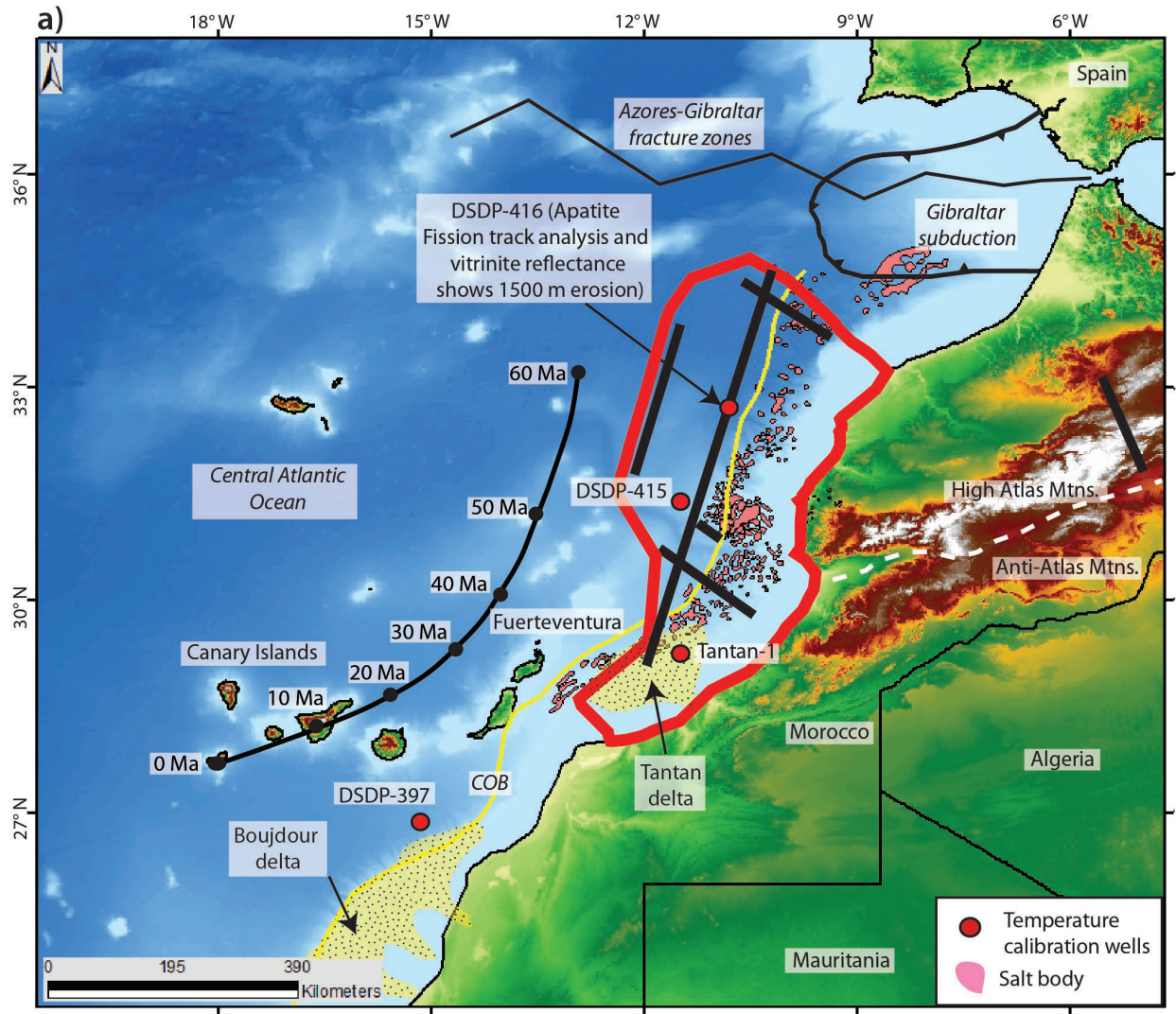


Figure 2. From Hasan (2022). Topographic map of northwestern Africa showing the location of the seismic lines, IODP and oil exploration wells, distribution of Jurassic salt bodies in pink, and the continent-ocean boundary shown as the yellow line; and the Canary Islands hotspot track that has been active from 60 Ma to the present-day.

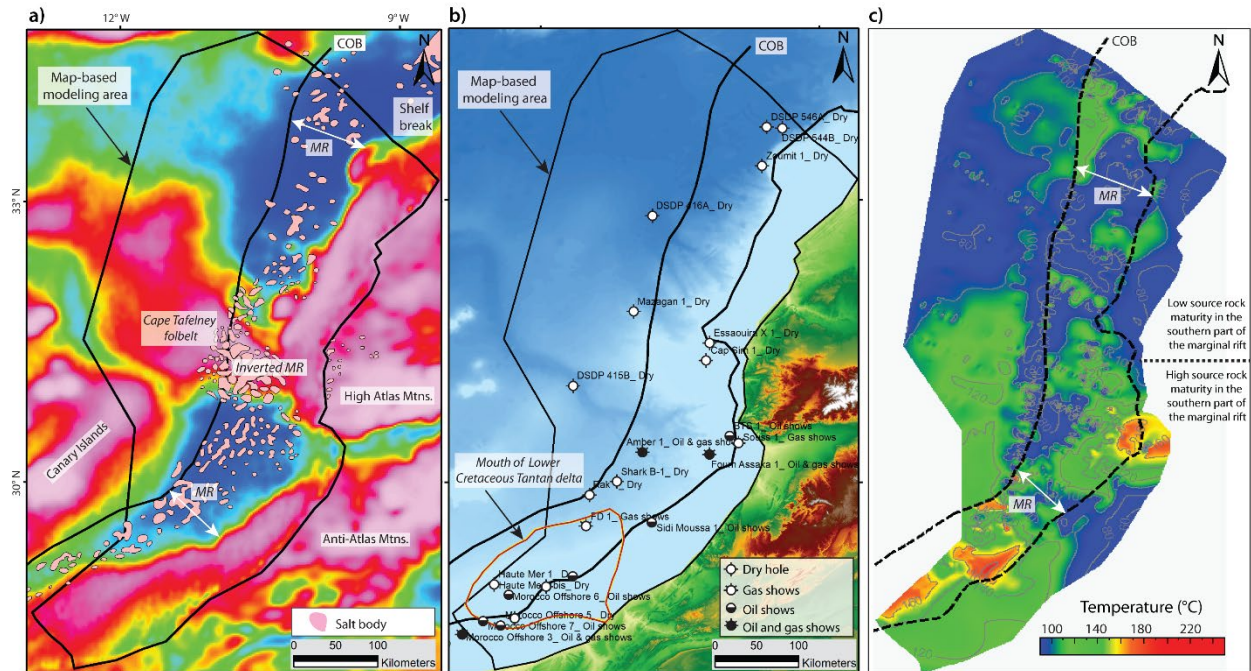


Figure 3. From Hasan (2022). A) Free-air gravity low corresponding to the 50-80-km-wide, Moroccan marginal rift that parallels the continent-oceanic boundary between the African continent and oceanic crust of the Central Atlantic Ocean Gravity highs include the High Atlas and Anti-Atlas mountains, that are areas of inverted Triassic-Jurassic rifts on thinned continental crust. B) Topographic and bathymetric map showing the location of existing drilling locations in the study area of the Moroccan marginal rift and their current status as producing wells, wells with shows, or dry holes (Beicip-Franlab (2019). C) Thermal maturity map based on our 1-D thermal maturity modeling of the proven Lower Jurassic source rock in the offshore Moroccan margin. Our prediction of thermal maturity shows that the southern marginal rift area is mature for hydrocarbon generation in contrast to the northern area, which remains immature. A clear correlation can be observed between the maturity prediction from the 1-D basin model and oil and gas, with the assumption that all the hydrocarbons are derived from Jurassic source rocks.

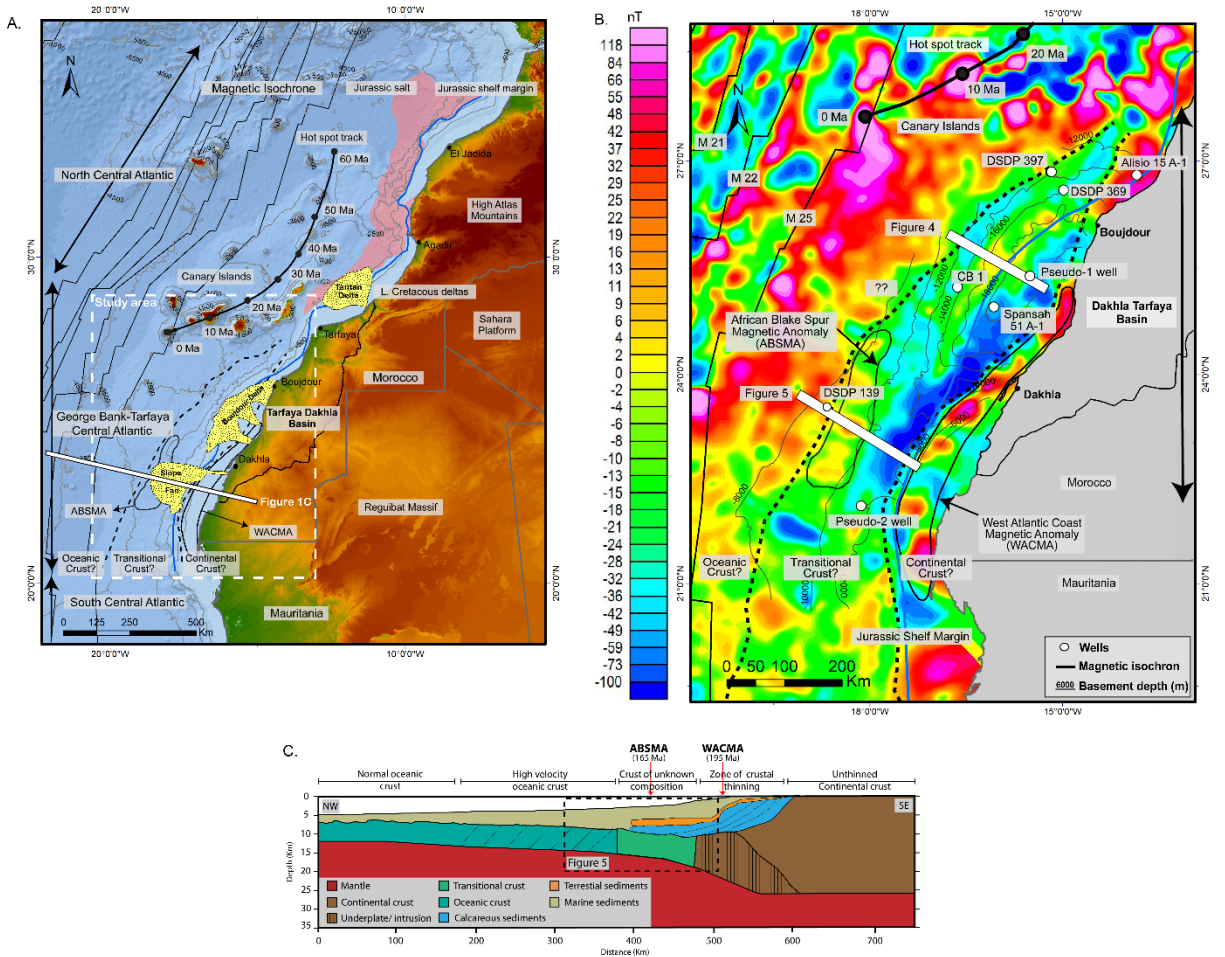


Figure 4. Figure from Galhom et al. (2022). **A.** Regional crustal framework of the Moroccan Atlantic rifted-passive margin showing its three major rifted-passive margin segments that are conjugate with eastern Canada: 1) Northern Central Atlantic; 2) Georges Bank- Tarfaya Central Atlantic, and; 3) South Central Atlantic (three zones are modified from Nemcok et al., 2005). The dashed white box shows the study area located within the Georges Bank-Tarfaya Central Atlantic segment of the Morocco rifted-passive margin. Oceanic crust of the central Atlantic Ocean is shown with early Cretaceous magnetic anomalies from Labails and Olivet (2009). The zone between the dashed black lines is rifted transitional crust based on the refraction line by Klingelhoefer et al. (2009) that is shown in Figure 1C. The blue line represents the seaward edge of the Jurassic carbonate shelf margin extension offshore Morocco from ONHYM (2019) and this study. The light red polygon in the north represents the extent of Jurassic salt along the northern Morocco margin from Tari et al. (2012). The black curved line with ages represents the Canary hot spot track (black dots) from 60 Ma to the present from Neumaier et al. (2016). **B.** Regional magnetic anomaly map of the Tarfaya Dakhla segment of the Moroccan rifted-passive margin shown by the area outlined by the dashed white lines in A. Magnetic data was compiled from the EMAG v. 3 global magnetic dataset from Meyer et al. (2017). Contour data represents top continental basement contours from this study. A broad magnetic high parallel to the Morocco shoreline includes the West Atlantic Coast Magnetic Anomaly (WACMA) as defined by Labails and Olivet (2009). The African Blake spur Magnetic Anomaly (ABSMA) is located 75 km to the west, as defined by Sahabi et al. (2004). The anomalous magnetic low parallel to the coastline represents a deeply subsided, continental basement with up to 19 km of sediment thickness that was named the Cape Boujdour marginal rift by Von Rad and Einsele (1980). The anomalous magnetic high at 300 km to the west corresponds to a broad, elongated basement high extending in a northeast-southwest direction between the Canary Islands in the north and Cape Verde in the south as described by Holik et al. (1991). Crustal interpretation to the area of queried crustal types is from

Klingelhofer et al. (2009). Crustal interpretation in the north to the area of queried crustal types is based on the compiled magnetic data and seismic profile in Galhom et al. (2022). C. Offshore-onland transect of the Moroccan Atlantic rifted-passive margin in the Dakhla area based on refraction and gravity modeling by Klingelhofer et al. (2009) (location of the cross-section is shown on the map in A). The section distinguishes five crustal types based on differences in seismic velocity, density, and top basement roughness; 1) Full-thickness continental crust. 2) Thinned continental crust 3) Zone of transitional crust of unknown composition. 4) High-velocity oceanic crust. 5) Normal oceanic crust.

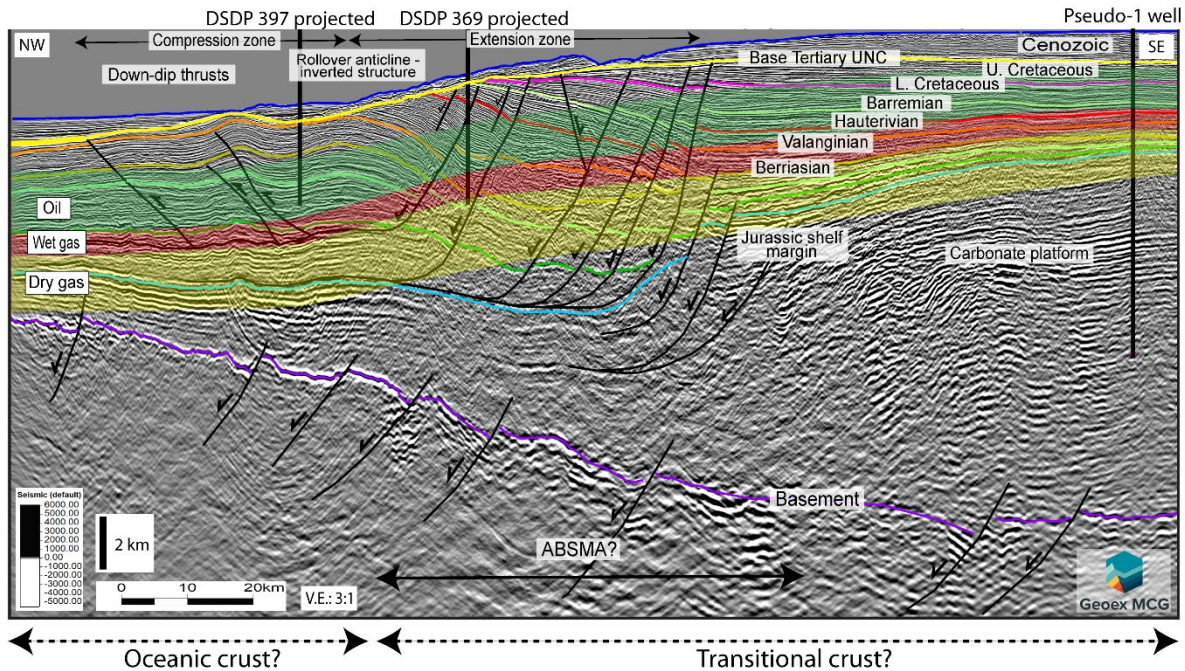


Figure 5. A) Regional 2D seismic profile across the study area summarizing the extent and depth ranges of the modeled windows for present-day oil, wet gas, and dry gas windows that are based on estimates using modeled vitrinite reflectance values from DSDP well 397, DSDP 369, Pseudo-1 well and Pseudo-2 well. The oil window is interpreted as 0.6–1.1 R_o , the wet gas window as 1.1–1.3 R_o , and the dry gas window as 1.3–2.0 R_o . These maturity windows are found at greater depths below the seafloor in the deeper water areas of the study area because of crustal heat flow is lower in areas of oceanic crust, and colder bottom waters are present at those greater water depths. Seismic data courtesy of Geox MCG.

16. Crustal structure and hydrocarbon potential of the non-volcanic and volcanic, rifted-passive margins of Mauritania

Md Upal Shahriar, PhD Candidate, University of Houston

This study describes the tectonostratigraphic evolution of the Mauritanian continental margin, an emerging hydrocarbon area on the margin of northwestern South America. This region was formed by the convergence of three tectonic elements: the continental crust of the West African craton, the rifted continental crust that underlies Mauritania's coastal area, shelf, and slope, and the Jurassic oceanic crust in the ultradeep area of the Central Atlantic Ocean, which includes the Miocene to recent Cape Verde hotspot (Figure 1). I use gravity filters to reveal the continent-ocean boundary (COB) and its marginal rifts and gravity modeling to show the transition in the width of the necking zone from the non-volcanic margin of Mauritania to the volcanic margin of Guinea Plateau. I also interpret dip and strike-oriented seismic sections along the study area to investigate the variation in crustal structure, stratigraphy, the extent of the syn-rift volcanic deposits, and the Moho depth (Figure 2). Seismic 2D depth structure maps were produced to show the extent and shape of the horizon and identify the margin's deepest part and the presence of marginal rifts. The tilt derivative gravity map revealed a band of thicker proto-oceanic crust parallel to the continent-ocean boundary. The oceanic crust is characterized by flexure beneath the continental margin, with landward dipping normal faults and a seaward flexural bulge. Regional strike lines show that the Guinea Plateau forms a localized volcanic margin related to a point source Jurassic hotspot. The Jacksonville fracture zone forms the abrupt northern edge of this volcanism. Therefore, almost all of Mauritania is non-volcanic and unaffected by widespread volcanism, implying that the Jurassic source rocks are sedimentary in the non-volcanic segment, which would increase their hydrocarbon source potential. The passive margin remained a carbonate margin from the Jurassic to the Cenomanian period, when it was terminated by an influx of clastic deltas and submarine fans in the late Cretaceous and Cenozoic. DSDP wells reveal that hydrocarbons and mature source rocks are extensive on the oceanic crust and become deeply buried by prograding submarine fan systems shown in Figure 3.

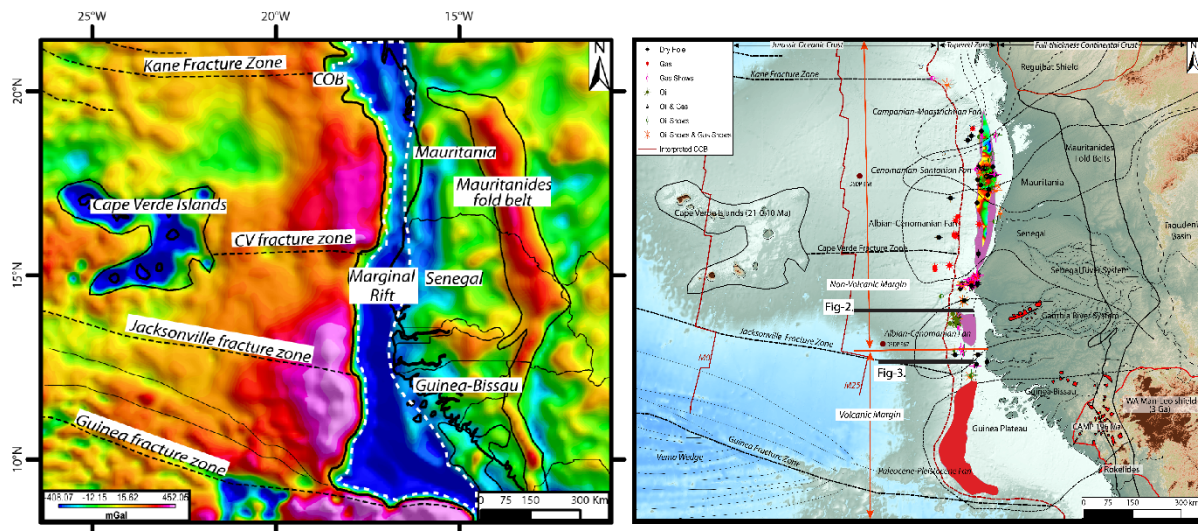


Figure 1. A) Vertical derivative of Bouguer gravity anomaly for the study area, showing the outline of the marginal rift along the rifted passive margin and the location of the COB. Heavy red line shows location of gravity model shown in the next figure. B) The salt and clastic sediment-filled marginal rift of the non-volcanic margin of northern and central Mauritania is shown in purple. To the south along the Guinea Plateau the marginal rift is filled by volcanic rocks that are shown in red. Drilling has shown that hydrocarbons are more commonly associated with the sedimentary marginal rift of the non-volcanic margin. Large fans blanket both the volcanic and non-volcanic margin.

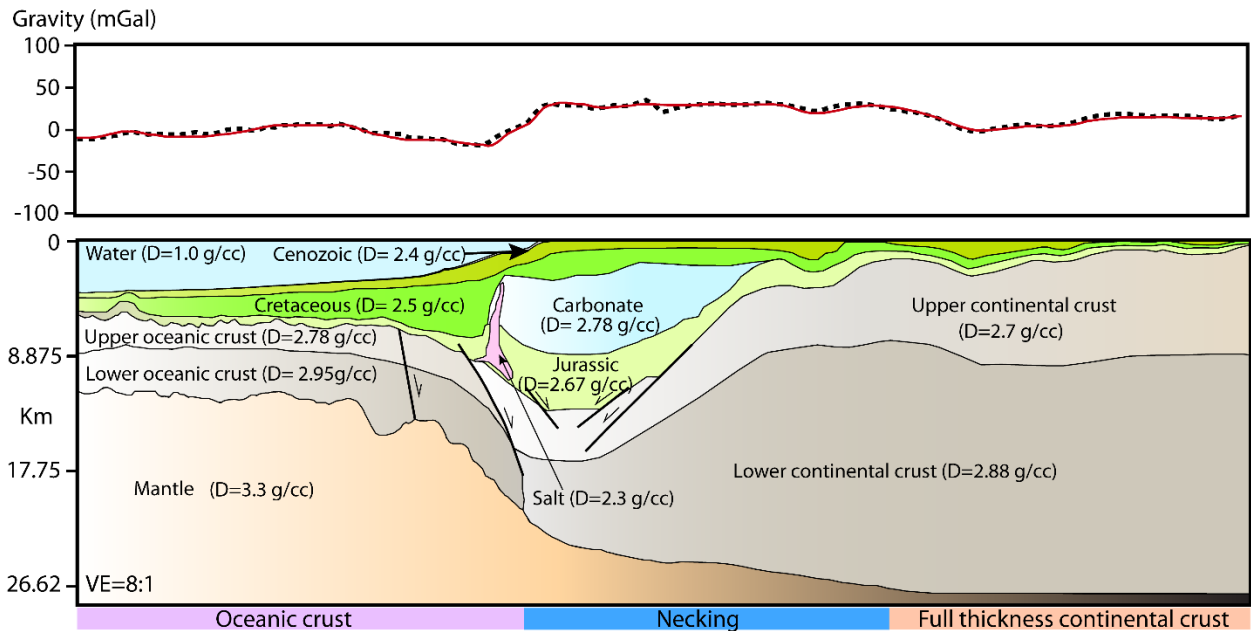


Figure 2. Seismic constrained gravity modeling of a line from Senegal margin. The onshore part is extrapolated based on the top of basement and sediment thickness data.

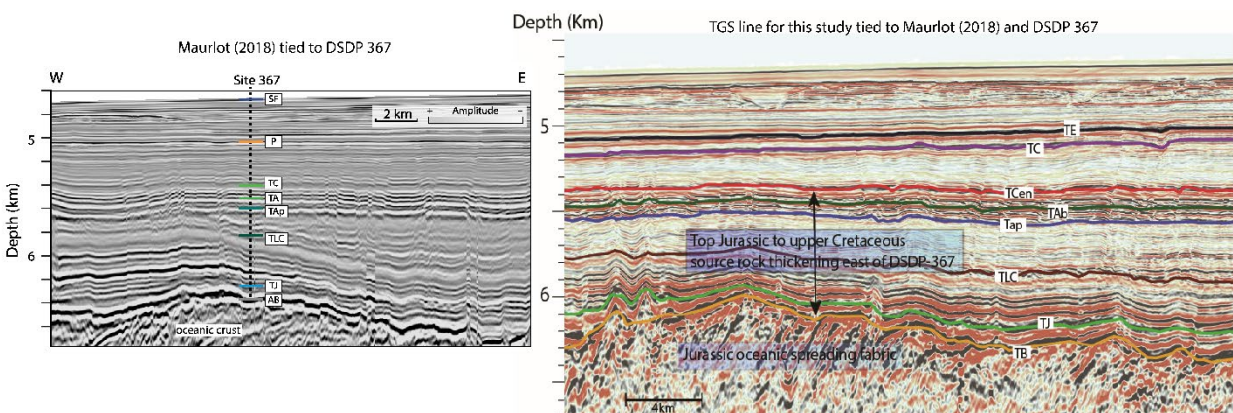


Figure 3. A) Seismic tie of TGS lines to DSDP 368 where mature Jurassic and Cretaceous source rocks are present. B) Line to right shows thickening of these source rocks in the landward direction where they are deeply buried by submarine fans.

17. Hydrocarbon prospectivity of deeply-buried Early Cretaceous rifts of the western deepwater area of the Niger delta, Nigeria

Jumoke Akinpelu, PhD Candidate, University of Houston

The Niger Delta basin is a prolific hydrocarbon province with the greater part of the exploration and production efforts concentrated on shallow, Cenozoic plays within the onshore delta area and in water depths ranging from shelfal to 1500 m. My study focuses on the potential of exploring new plays into ultra-deep waters (>1500m) and at deeper depths for Cretaceous rift plays now buried by the deepwater, western extent of the Niger delta (Figure 1). Analogs to this type of discovery are based on Aptian, rift-related source rocks are documented along the Gulf of Guinea offshore Ghana (Jubilee Field, Tano basin), Sierra Leone and Liberia (Venus and Mercury Discoveries) (Figure 1). Other sources that have been described include the Cenomanian-Turonian interval in the overlying passive margin section.

Morgan (2003) has described deeply buried Aptian rifts on the seismic line shown in Figure 2. My proposed deep hydrocarbon prospect assumes an Aptian source as described by Dailly (2017) in successful wells to the west of this area (Figure 1), reservoirs within the rift, and seals based on the deltaic cover this section. To support this hypothesis, I will better characterize the crustal structure and heat flow using gravity and magnetic data; carry out mapping of more modern and deeply-penetrating seismic data; carry out geochemical characterization of potential source rocks based on regional data from previous works and available sources, and create standard thermal stress (STS) maps based on constant radiogenic heat production (RHP) and expelled hydrocarbons maps for the study area, as well as a 1D basin modeling of pseudo wells placed in critical areas..

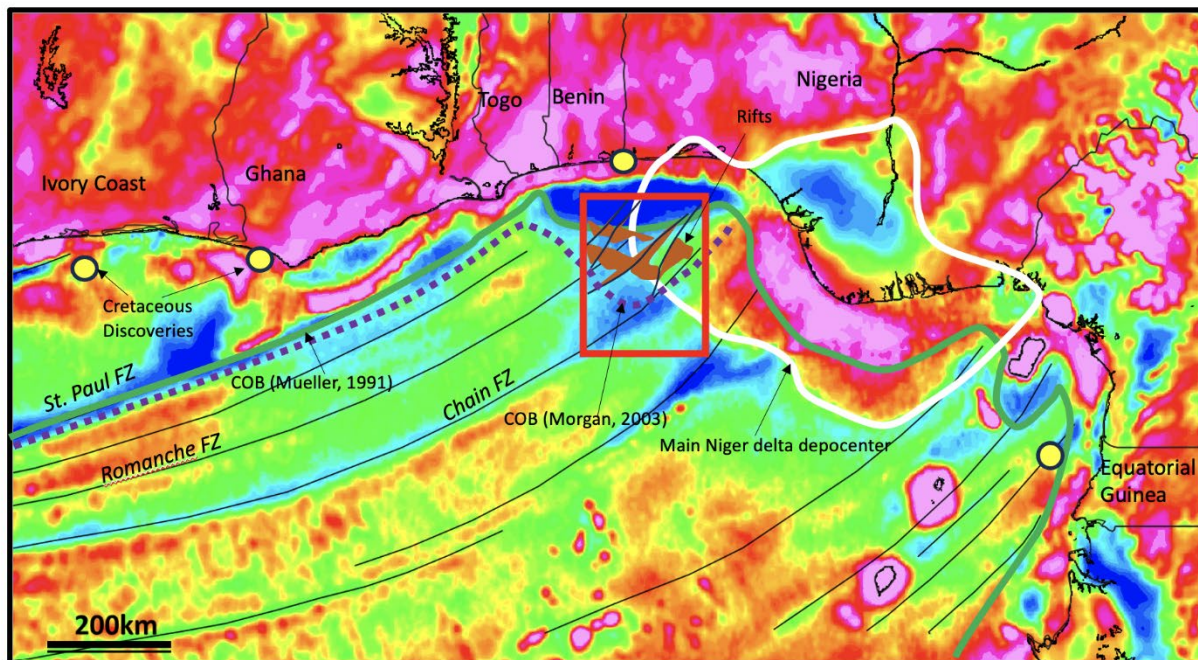


Figure 1. Satellite-derived, free-air gravity map from Sandwell et al. (2014) showing the main depocenter of the Niger delta outline by the heavy white line, fracture zones as thin black lines in oceanic crust that were precisely mapped from satellite data by Steier (2016), and yellow dots show the locations of rift-related Cretaceous source rock-based discoveries described by Dailly et al. (2017). The red box shows the study area of Morgan (2003), where he defined the continent-ocean boundary (dashed line) separating deeply-buried Aptian rifts shown by brown polygons overlain by prograding shale and sand of the Niger delta. The green line is the continent-ocean boundary previously proposed by Nürnberg and Müller (1991) using only satellite data. Note that the Morgan (2003) COB extends further seaward than the Nürnberg and Müller (1991) interpretation and enlarges the play fairway for rift-related source rocks. Location of the seismic line from Morgan (2003) in Figure 2 is indicated.

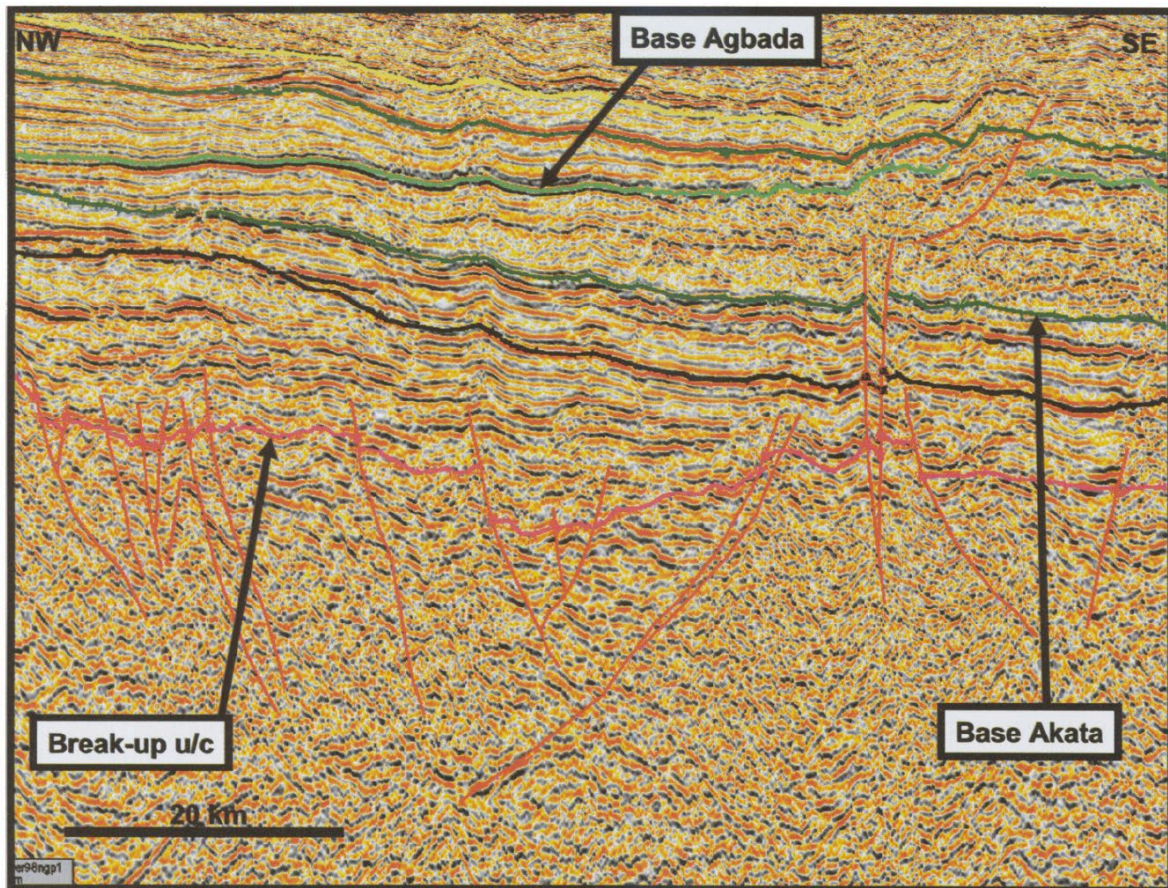


Figure 2: Seismic lines from Morgan (2003) showing 1.5 km of syn-rift fill. An unconformity, angular in places, divides the syn-rift from the post-rift fill. A presumed Late Cretaceous sediment apron overlies the rift-fill succession, indicating significant sediment delivery to this part of the margin during this phase. These sediments are in turn onlapped by the Akata Formation seismic facies, which thins to the north. A second phase of shelf-slope build-out centered on the Dahomey Embayment follows the Akata deposition. This is correlated with the lowermost part of the Agbada Formation. I infer that mature source rocks may be present in the rift and with strong seals and will test this with basin modeling.

18. 3D and 2D mapping and basin modeling of the Rio Muni Basin, offshore Equatorial Guinea

José Miguel Gorosabel Araus, Research Associate 1, University of Houston

The Rio Muni Basin is an offshore petroleum province located in the Gulf of Guinea in West Africa. It comprises a region between the equatorial and central segments of the South Atlantic, between the Niger Delta and the North Gabon Basin. The basin was formed during the diachronous, northward-propagating rifting of Gondwana during the Early Cretaceous and developed as an oblique margin with stretching and rifting of continental crust before the breakup (Figure 1).

Two oil fields have been developed in the proximal domain of the basin, the Okume complex and the Ceiba field (West African play), with a production of 81,000 barrels of oil per day (bopd) for the Okume complex (cumulative production of 205 million barrels) and 2,400 bopd for the Ceiba field from high-quality Upper Cretaceous sands. The proposed petroleum systems in the basin include source rock intervals deposited during the Early Cretaceous, Late Cretaceous, and Paleogene.

Although syn-rift and transitional source rocks of the continental margin are not expected in the distal basin setting on oceanic crust, prolific Turonian source rocks are proposed, together with Paleogene source intervals. Despite the oceanic nature of the crust, geochemical fingerprinting of oil seeps recovered on the islands of São Tomé and Príncipe has proved the Cretaceous origin of samples (Figure 1), which might indicate the maturation of this level resulted from a thick overburden of sediments (up to 5 sTWT).

Our study is based on the interpretation of 5 3D seismic blocks and 43 2D seismic lines (provided by Geox MCG) and their integration with gravity data, magnetic data, and structural and crustal models (Figure 1). The research has been divided into 2 phases. The first stage involves mapping the petroleum system's principal elements and the basin's structural analysis. The results will be integrated with geothermal data and crustal models to complete the basin modeling of the area of interest (AOI, Figure 1).

Preliminary results indicate the presence in the basin of potential source rocks for the Cretaceous, together with turbidite and contourite deposits as proposed reservoirs. While Aptian evaporites might represent the seal in the proximal margin, transgressive shales could act as potential seals in the deep oceanic domain. Downslope gravitation complexes and salt-related deformation might have played an essential role in the development of traps in the proximal segment of the basin. The oceanic crust is characterized by the presence of deformation related to the development of the Cameroon Volcanic Line. The episodic deformation of the oceanic crust and the overlying sedimentary section has led to the development of potential structural, stratigraphic, and combination traps.

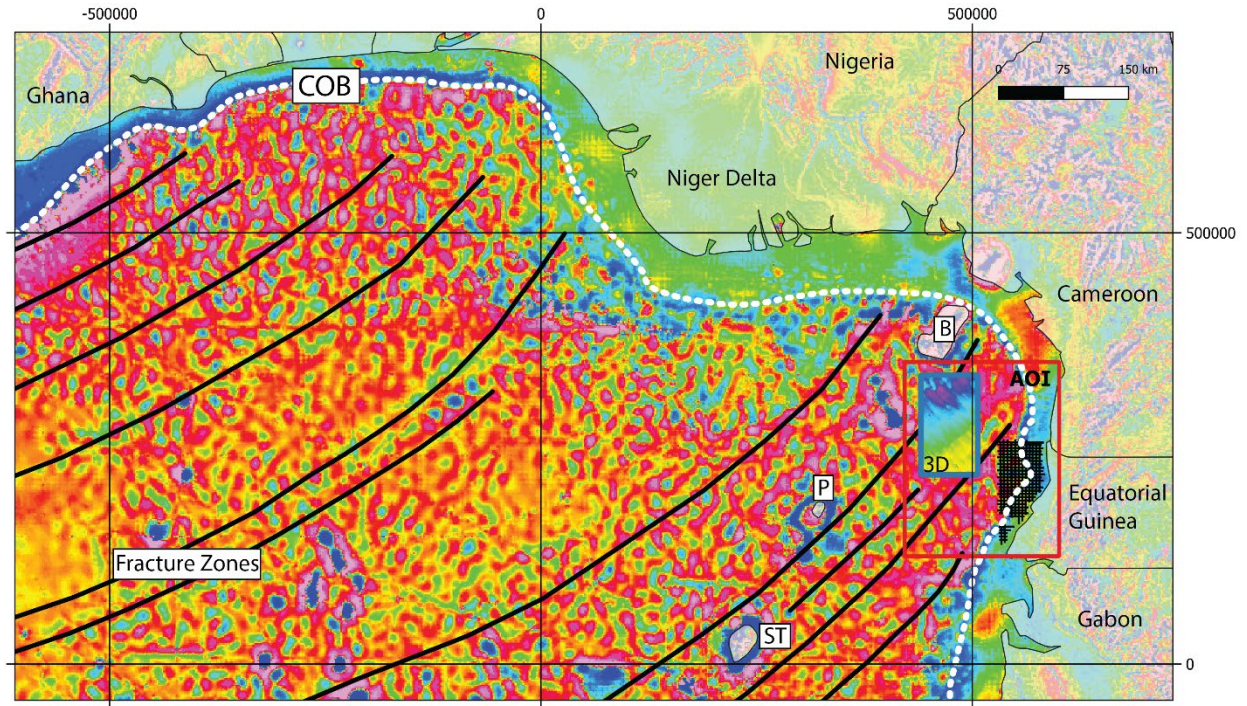


Figure 1. Seismic data provided by Geox MCG for this study. Top of basement interpretation given for the 3D seismic dataset. Key to acronyms: B, Bioko Island; P, Principe Island; ST, Sao Tome Island; COB, Continental - Oceanic Boundary.

19. Relationships between Red Sea opening directions, crustal types and thicknesses, evaporite distribution, and hydrocarbon potential

Mohamed Abdelfatah, PhD Candidate, University of Houston

The 2000-km-long and 200-350-km wide Red Sea Rift began to form in the Oligocene as Precambrian continental crust of the Arabian Peninsula separated from northeastern Africa. Previous GPS studies have shown that the northern rift in Egypt and Arabia rifts obliquely to the NNE at a slower rate of 6.8 mm/yr compared to the central and southern rift in Sudan, Arabia, Eritrea, and Yemen that rifts orthogonally to the NE at a faster rate of 15.7 my/yr (Figure 1). This tectonic setting provides the opportunity for understanding how these systematic variations in rift opening directions and rates are manifested in the longer-term and along-strike changes in the crustal structure and structural style of the Red Sea. Because the Red Sea is one of the few actively forming Cenozoic rifts on Earth, our objective is to describe how these along-strike crustal and structural changes can serve as a template for understanding older and more deeply-buried continental rifts.

We use the following data types to describe the Red Sea crustal structure and structural style: 1) publicly-available bathymetric, gravity, and magnetic data to understand crustal structure including the distribution of continental and oceanic crust; and 2) 10,919 line-km of industry, multi-channel seismic reflection data tied to exploration wells in the Egyptian sector of the northern Red Sea to understand structural style of the rifted areas; and 3) compilation of previous seismic reflection studies and wells from Arabia, Sudan and Eritrea that provide information on the rift structural style in these areas. The main findings include: 1) the northern Red Sea north of the left-lateral Zabargad fracture zone is a zone of continental rifting with a central main rift axis that is diagonal to the overall Red Sea; domino-style normal faults dip inward to the elongate trough of the main rift axis; normal faults are commonly disrupted by transfer faults; Miocene salt flows into the trough along the main rift axis (Figure 2); 2) the southern Red Sea south of the ZFZ exhibits a transition from continental rifting to a young, oceanic spreading center flanked by a narrow strip of oceanic crust; trends of the rifts and spreading center are parallel to the overall trend of the Red Sea and are less disrupted by transfer faults; the axial valley of the spreading ridge is elevated and controls a landward flow of Miocene syn-rift and pre-oceanic Miocene salt; in most areas the widening area of young oceanic crust in the southern Red Sea splits the once continuous, pre-rift salt body into two separate salt bodies. Our proposed sub-salt hydrocarbon plays for the Red Sea are similar to the discoveries in the Gulf of Suez and consist of syn-rift source rocks and clastic reservoir sections sealed by the overlying salt sheet.

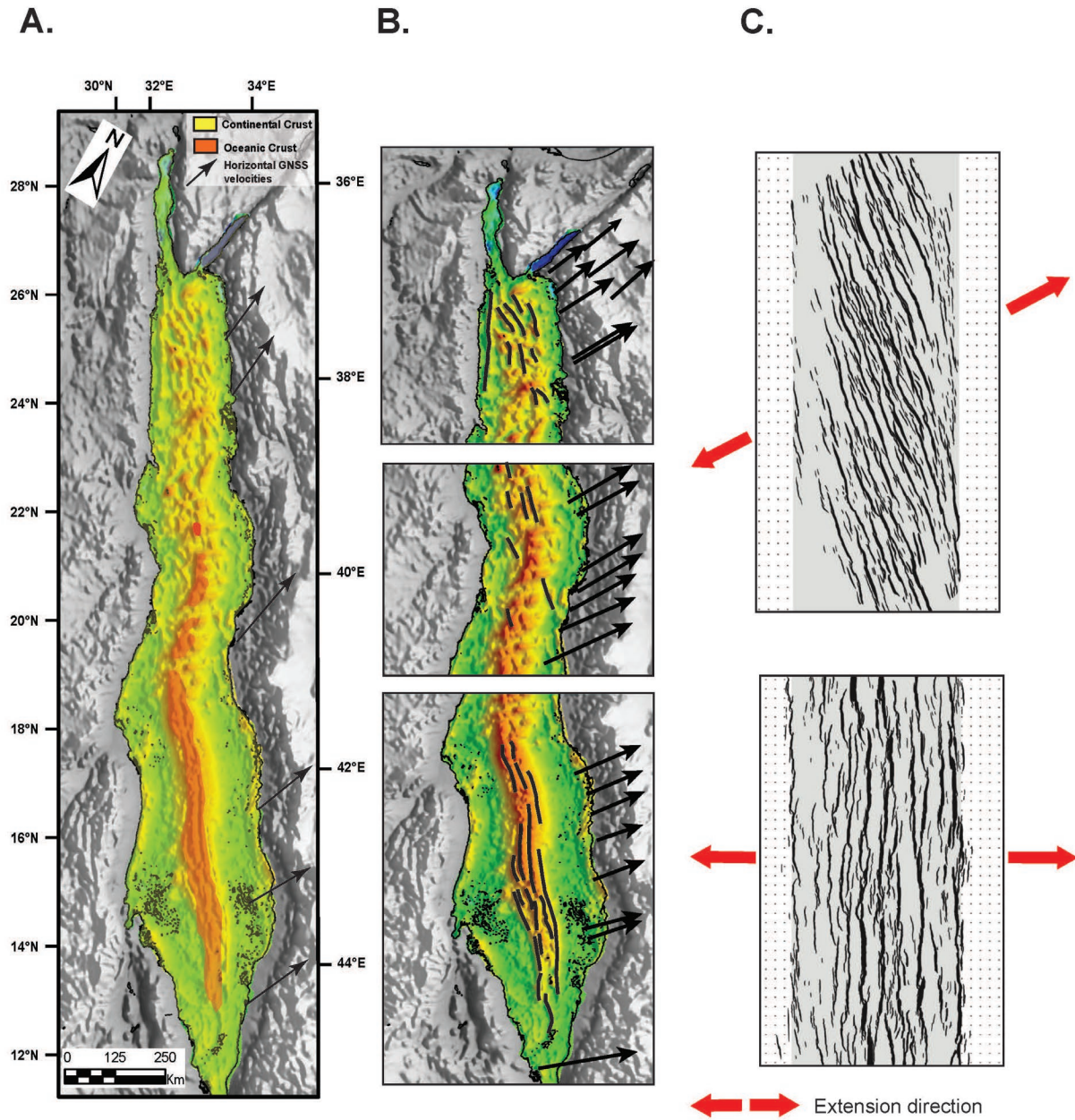


Figure 1. A) Bouguer gravity map of the Red Sea showing the disrupted basement with oblique trends in the continental rift zone in the northern Red Sea that contrasts with the lineated and continuous areas of oceanic crust forming orthogonally along an oceanic spreading ridge in the southern Red Sea. B) Transfer faults are more common in the more disrupted area of continental rifting. Arrows are GPS vectors from ArRajehi et al. (2010) show changes in the rate and direction of Red Sea opening from north to south. C) Clay modeling experiments by Withjack et al. (2002) showing oblique trends formed in obliquely-opening rifts compared to basin-parallel trends formed in orthogonally-opening rifts.

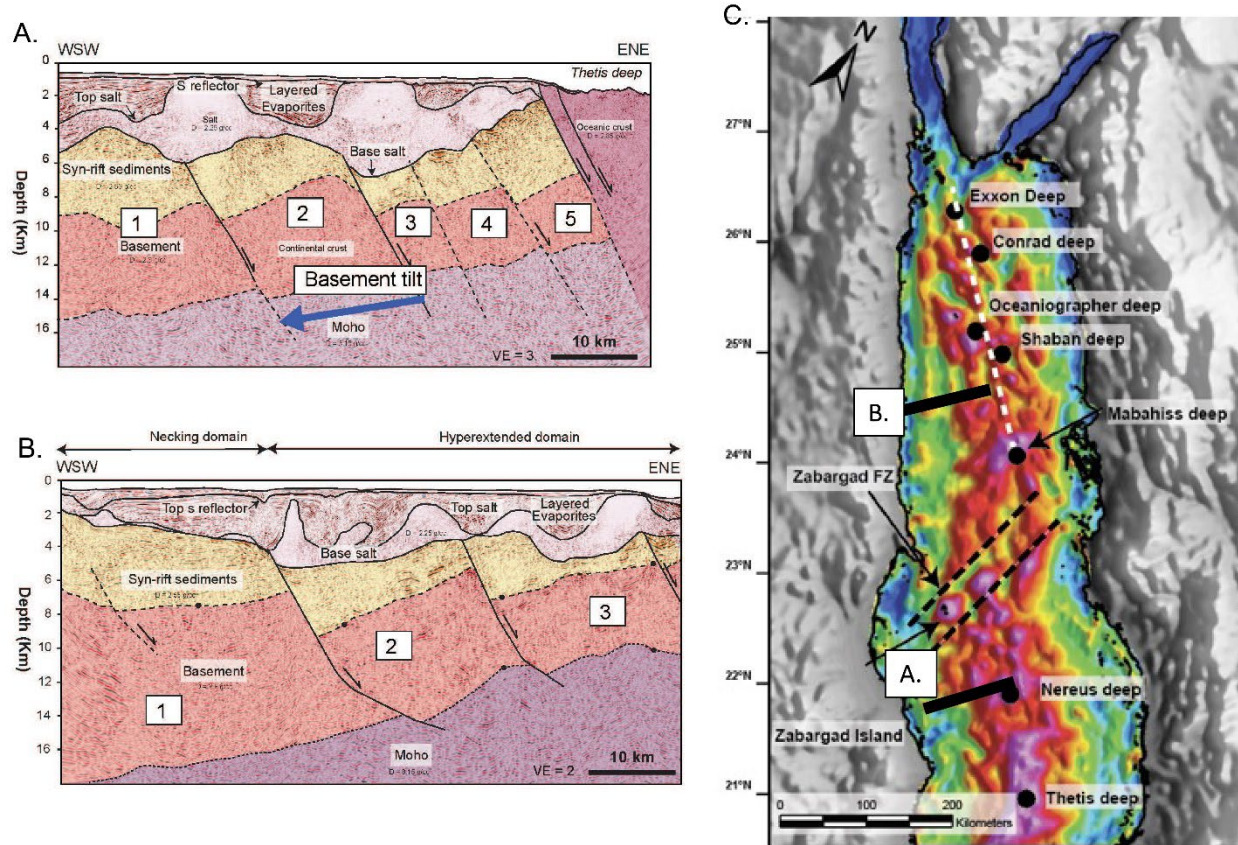


Figure 2. A) Interpretation of TGS seismic reflection line showing domino-style, rotated fault blocks 1-5 adjacent to young oceanic crust at the Thetis deep. Pink is salt with overlying clastic minibasins controlled by salt movement, yellow is syn-rift sedimentary rocks, red is crystalline basement rocks, and purple is the upper mantle. Note thickening of salt in the half-grabens and absence of salt above young oceanic crust of the Thetis deep. B) Interpretation of TGS seismic reflection line from the Egyptian section of the northern Red Sea showing domino-style, rotated fault blocks 1-3 with same color coding as A. C) Gravity map showing the locations of seismic lines A and B.

REFERENCES

- Adams, D.C. and Keller, G.R., 1996, Precambrian basement geology of the Permian Basin region of west Texas and eastern New Mexico: A geophysical perspective, *AAPG Bulletin*, v. 80, no. 3, p. 410–431. <https://doi.org/10.1306/64ED87FA-1724-11D7-8645000102C1865D>
- Allen, P.A., and Allen, J.R., 2013, *Basin analysis: principles and application to petroleum play assessment* (third ed.), Wiley-Blackwell, p. 632.
- ArRajehi, A., McClusky, S., Reilinger, R., Daoud, M., Alchalbi, A., Ergintav, S., et al., 2010, Geodetic constraints on present-day motion of the Arabian Plate: Implications for Red Sea and Gulf of Aden rifting, *Tectonics*, v. 29, no. 3, TC3011. <https://doi.org/10.1029/2009TC002482>
- Ballard, J., 2019, Delineation of Submarine Fan Systems in the Guyana/Suriname Basin, Unpublished. https://www.researchgate.net/publication/339365381_Delineation_of_Submarine_Fan_Systems_in_the_GuyanaSuriname_Basin
- Beicip-Franlab, 2019, Thermal and maturity modeling of Nova Scotia and northern Morocco conjugate margins. p. 33. Accessed on September 22, 2022. https://oera.ca/sites/default/files/2020-03/Chapter5_Basin_Modelling_FINAL.pdf
- Bugti, M.N., 2022, Mesozoic plate reconstruction, salt tectonics, and hydrocarbon potential of the western Gulf of Mexico basin, PhD dissertation, University of Houston, 221 p.
- Carvajal-Arenas, L.C., Torrado, L., Mann, P., and English, J., 2020, Basin modeling of Late Cretaceous / Mio-Pliocene petroleum system of the deep-water eastern Colombian Basin and South Caribbean Deformed Belt: Marine and Petroleum Geology, v. 121, p. 104511. <https://doi.org/10.1016/j.marpetgeo.2020.104511>
- Chauvet, F., Sapin, F., Geoffroy, L., Ringenbach, J.C., and Ferry, J.N., 2021, Conjugate volcanic passive margins in the austral segment of the South Atlantic—Architecture and development, *Earth-Science Reviews*, v. 212, 103461. <https://doi.org/10.1016/j.earscirev.2020.103461>
- Dailly, P., Henderson, T., Kanschat, K., Lowry, P., and Sills, S., 2017, Chapter 14: The Jubilee Field, Ghana: Opening the Late Cretaceous Play in the West African Transform Margin, in R.K. Merrill and C.A. Sternbach, eds., *Giant Fields of the Decade 2000-2010*, AAPG Memoir, v. 113, p. 257-272. <https://doi.org/10.1306/13572010M1132997>
- DeVito, S., and Kearns, H., 2022, Overview of the exploration potential of offshore Argentina – insight from new seismic interpretations, *Petroleum Geoscience*, v. 28, no. 2. <https://doi.org/10.1144/petgeo2020-132>
- Dressel, I., Scheck-Wenderoth, M., and Cacace, M., 2017, Backward modelling of the subsidence evolution of the Colorado Basin, offshore Argentina and its relation to the evolution of the conjugate Orange Basin, offshore SW Africa, *Tectonophysics*, v. 716, p. 168-181. <https://doi.org/10.1016/j.tecto.2016.08.007>
- Erlich, R.N., and Pindell, J., 2020, Crustal origin of the West Florida Terrane, and detrital zircon provenance and development of accommodation during initial rifting of the southeastern Gulf of Mexico and western Bahamas, *Geological Society, London, Special Publications*, v. 504, p. 77-118. <https://doi.org/10.1144/SP504-2020-14>
- Escalona, A., Norton, I., Lawver, L., and Gahagan, L., 2021, Quantitative plate tectonic reconstructions of the Caribbean region from Jurassic to present, in C. Bartolini (ed.), *South America-Caribbean-Central Atlantic Plate Boundary: Tectonic Evolution, Basin Architecture, and Petroleum Systems*, AAPG Memoir 123, p. 239–264. <https://doi.org/10.1306/13692247M1233849>
- Ewing, T.E., Barnes, M.A., and Denison, R.E., 2019, Proterozoic foundations of the Permian Basin, West Texas and southeastern New Mexico— a review, in Ruppel, S. C., ed., *Anatomy of a Paleozoic*

- basin: the Permian Basin, USA, (vol. 1, ch. 3), The University of Texas at Austin, Bureau of Economic Geology Report of Investigations 285; AAPG Memoir, v. 118, p. 43–61.
- Galhom, T., Mann, P., and Rudolph, K., 2022, Jurassic-Recent structure, stratigraphy, and basin modeling of the rifted-passive margin of the Tarfaya-Dakhla basin of southern Morocco, *Marine and Petroleum Geology*, 105626. <https://doi.org/10.1016/j.marpetgeo.2022.105626>
- Hasan, M.N., 2022, Tectonostratigraphy, structural styles, and hydrocarbon prospectivity of the rifted-passive margins of the southern Gulf of Mexico and the Atlantic margin of Morocco, PhD dissertation, University of Houston, 265 p.
- Holik, J.S., Rabinowitz, P.D., and Austin, J.A., 1991, Effects of Canary hotspot volcanism on structure of oceanic crust off Morocco, *Journal of Geophysical Research*, v. 96, p. 12039–12067. <https://doi.org/10.1029/91jb00709>
- Horne, E., Hennings, P., and Zahm, C., 2021, Basement-rooted faults of the Delaware Basin and Central Basin Platform, Permian Basin, West Texas and southeastern New Mexico, in Callahan, O.A., and Eichhubl, P., *The Geologic Basement of Texas: A Volume in Honor of Peter T. Flawn: The University of Texas at Austin, Bureau of Economic Geology Report of Investigations No. 286*, 37 p. <http://dx.doi.org/10.23867/RI0286C6>
- Klingelhoefer, F., Labails, C., Cosquer, E., Rouzo, S., Geli, L., Aslanian, D., et al., 2009, Crustal structure of the SW-Moroccan margin from wide-angle and reflection seismic data (the DAKHLA experiment) Part A : wide-angle seismic models, *Tectonophysics*, v. 468, p. 63–82. <https://doi.org/10.1016/j.tecto.2008.07.022>
- Labails, C., Olivet, J.-L., Aslanian, D., and Roest, W.R., 2010, An alternative early opening scenario for the Central Atlantic Ocean, *Earth and Planetary Science Letters*, v. 297, p. 355–368. <https://doi.org/10.1016/j.epsl.2010.06.024>
- Ladd, J.W., and Sheridan, R.E., 1987, Seismic stratigraphy of the Bahamas, *AAPG Bulletin*, v. 71, no. 6, p. 719–736. <https://doi.org/10.1306/94887898-1704-11D7-8645000102C1865D>
- Leslie, S., and Mann, P., 2020, Structure, stratigraphy, and petroleum potential of the deepwater Colombian basin, offshore northern Colombia, *Interpretation*, v. 8, n. 4, p. 1N-T1095. <https://doi.org/10.1190/INT-2020-0028.1>
- Liang, W., Li, J., Xu, X., Zhang, S., and Zhao, Y., 2020, A High-Resolution Earth's Gravity Field Model SGG-UGM-2 from GOCE, GRACE, Satellite Altimetry, and EGM2008, *Engineering*, v. 6, no. 8, p. 860–878. <https://doi.org/10.1016/j.eng.2020.05.008>
- Lin, P., Bird, D., and Mann, P., 2019, Crustal structure of an extinct, late Jurassic-to-earliest Cretaceous spreading center and its adjacent oceanic crust in the eastern Gulf of Mexico: *Marine Geophysical Research*, v. 40, p. 395–418. <https://doi.org/10.1007/s11001-019-09379-5>
- Liu, M., 2021, Mesozoic rift evolution and crustal structure of the Gulf of Mexico Basin from integration of multiple geological and geophysical datasets, PhD dissertation, University of Houston, 219 p.
- Meyer, B., Chulliat, A., and Saltus, R., 2017, Derivation and error analysis of the Earth magnetic anomaly grid at 2 arc min resolution: Version 3 (EMAG2v3), *Geochemistry, Geophysics, Geosystems*, v. 18, no. 12, p. 4522–4537. <https://doi.org/10.1002/2017GC007280>
- Morgan, R., 2003, Prospectivity in ultradeep water: the case for petroleum generation and migration within the outer parts of the Niger Delta apron, *Geological Society of London, Special Publications*, v. 207, p. 151-164. <https://doi.org/10.1144/GSL.SP.2003.207.8>
- Neumaier, M., Back, S., Littke, R., Kukla, P.A., Schnabel, M., and Reichert, C., 2016, Late Cretaceous to Cenozoic geodynamic evolution of the Atlantic margin offshore Essaouira (Morocco), *Basin Research*, v. 28, p. 712–730. <https://doi.org/10.1111/bre.12127>
- Nürnberg, D., and Müller, R.D., 1991, The tectonic evolution of the South Atlantic from Late Jurassic to present, *Tectonophysics*, v. 191, no. 1-2, p. 27-53. [https://doi.org/10.1016/0040-1951\(91\)90231-G](https://doi.org/10.1016/0040-1951(91)90231-G)
- Ong, E., 2023, The Atlantic Margin..... The Gift that keeps on giving, unpublished report on LinkedIn.

- ONHYM, 2019, Opportunities for hydrocarbons exploration and production in Morocco, Boujdour: handout, AAPG International Conference and Exhibition, May, 19-22, 2019, San Antonio, USA.
- Pollitt, D.A., and Sun, S., 2023, Exploration benchmarking to establish the potential of two hydrocarbon plays in the Pelotas and Punta del Este Basins, offshore Uruguay, AAPG Bulletin, v. 107, no. 5, p. 721-742. <https://doi.org/10.1306/09142221207>
- Price, L.M., Perkey, R.A., Oswald, E.J., and Elkington, E.A., 2021, Chapter 15: Liza Field, Guyana: The Finding of a Stratigraphic Giant, from Early Exploration to Production, in C.A. Sternbach, R.K. Merrill, and J.C. Dolson, eds., Giant Fields of the Decade: 2010-2020, AAPG Memoir, v. 125, p. 433-455. <https://doi.org/10.1306/13742366MGF.15.3882>
- Ramirez, V., Vargas, L.S., Rubio, C., Nino, H., and Mantilla, O., 2015, Petroleum systems of the Guajira Basin, northern Colombia, in C. Bartolini and P. Mann, eds., Petroleum geology and potential for the Colombian Caribbean margin: AAPG Memoir, v. 108, p. 399-430. <https://doi.org/10.1306/13531944M1083647>
- Reuber, K., Mann, P., and Pindell, J., 2019, Hotspot origin for asymmetrical, conjugate volcanic margins of the austral South Atlantic Ocean as imaged on deeply-penetrating seismic reflection images, Interpretation, v. 7, n. 4, p.SH71-SH97. <https://doi.org/10.1190/int-2018-0256.1>
- Rodríguez-Zurrunero, A., Granja-Bruña, J.L., Muñoz-Martín, A., Leroy, S., ten Brink, U., Gorosabel-Araus, J.M., Carbó-Gorosabel, A., 2020, Along-strike segmentation in the northern Caribbean plate boundary zone (Hispaniola sector): Tectonic implications, Tectonophysics, v. 776, 228322. <https://doi.org/10.1016/j.tecto.2020.228322>
- Rowan, M.G., 2022, The ocean-continent transition of late synrift salt basins: Extension and evaporite deposition in the southern Gulf of Mexico and global analogs, in C. Koeberl, P. Claeys, A. Montanari, eds., From the Guajira Desert to the Apennines, and from Mediterranean Microplates to the Mexican Killer Asteroid: Honoring the Career of Walter Alvarez, GSA Special Paper, v. 557. [https://doi.org/10.1130/2022.2557\(12\)](https://doi.org/10.1130/2022.2557(12))
- Sahabi, M., Aslanian, D., and Olivet, J.L., 2004, Un nouveau point de départ pour l'histoire de l'Atlantique central, Compt. Rendus Geosci. v. 336, p. 1041-1052. <https://doi.org/10.1016/j.crte.2004.03.017>
- Sandwell, D.T., Müller, R.D., Smith, W.H.F., Garcia, E., Francis, R., 2014, New global marine gravity model from CryoSat-2 and Jason-1 reveals buried tectonic structure, Science, v. 346, no. 6205, p. 65-67, <https://doi.org/10.1126/science.1258213>
- Sheridan, R.E., Crosby, J.T., Bryan, G.M., and Stoffa, P.L., 1981, Stratigraphy and structure of southern Blake Plateau, northern Florida Straits, and northern Bahama Platform from multichannel seismic reflection data, AAPG Bulletin, v. 65, no. 12, p. 2571-2593. <https://doi.org/10.1306/03B59A08-16D1-11D7-8645000102C1865D>
- Steier, A., 2016, Fine Tuning Quantitative, Plate-Tectonic Reconstructions of South Atlantic Conjugate Margins using a GIS Compilation of Geologic and Geophysical Information, 15th Houston Geological Society - Petroleum Exploration Society of Great Britain Conference on African E&P, Houston, Texas, Sept. 12-14, 2016.
- Tari, G., Brown, D., Jabour, H., Hafid, M., Loudon, K., and Zizi, M., 2012, The Conjugate Margins of Morocco and Nova Scotia, in Bally, B., et al., eds., Regional Geology and Tectonics: Phanerozoic Passive Margins, Cratonic Basins, and Global Tectonic Maps, Elsevier, p. 284-323. <https://doi.org/10.1016/B978-0-444-56357-6.00007-X>.
- Turrini, L., Jackson, C.A.L., and Thompson, P., 2017, Seal rock deformation by polygonal faulting, offshore Uruguay, Marine and Petroleum Geology, v. 86, p. 892-907. <https://doi.org/10.1016/j.marpetgeo.2017.06.038>
- Von Rad, U., Einsele, G., 1980, Mesozoic-cainozoic subsidence history and palaeobathymetry of the northwest african continental margin (Aaiun basin to DSDP site 397), Philosophical

- Transactions of the Royal Society of London, Series A, Mathematical, Physical, and Engineering Sciences, v. 294, p. 37–50. <https://doi.org/10.1098/rsta.1980.0010>
- Withjack, M., Schilsche, R., and Olsen, P., 2002, Rift-basin structure and its influence on sedimentary systems, Sedimentation in Continental Rifts, SEPM Special Publication, no. 73, p. 57-81. <https://doi.org/10.2110/PEC.02.73.0057>
- Zhang, H., Mann, P., Bird, D., and Rudolph, K., 2021, Integration of regional gravity modeling, subsidence analysis, and source rock maturity data to understand the tectonic and hydrocarbon evolution of the Permian Basin, west Texas, Interpretation, v. 9, n. 1, 1-F-Y1. <https://doi.org/10.1190/INT-2020-0065.1>



For more information, please visit our website at cbth.uh.edu

Or contact us via e-mail at cbthproject@gmail.com